NOVEL BIOFUNCTIONAL POLYESTER NANOFIBERS

by

Evrim Arslan

Integrated B.S. and M.S., Teaching Chemistry, Bogazici University, 2013

Submitted to the Institute for Graduate Studies in
Science and Engineering in partial fulfillment of
the requirements for the degree of
Master of Science

Graduate Program in Chemistry
Boğaziçi University

2016

Dedicated to my family

ACKNOWLEDGEMENTS

I would like to state my gratefulness to my supervisor Assoc. Prof. Amitav Sanyal to give me the opportunity to work in his research group. I would like to express my thanks to him for his support, scientific guidance through this project and endless attention. I gained lots of experience during half and one year.

I would like to extend my thanks to Assoc. Prof. Rana Sanyal for her scientific support and advices regarding my project.

I am so glad for meeting all the people in Sanyal Group and working with them. I wish to express my great thanks to Özlem İpek Kalaoğlu Altan for her support and guidance. Moreover, I want to thank Filiz Emlik Çalık for her helpfulness, kindness, cheerfulness and guidance on my thesis. I would like to thank Laura Chambre for her support and helpfulness. I would like to thank Gizem Yeter Baş, Azize Kıraç, Büşra Karagöz, Merve Karaçivi, Ülkü Güler, Tuğçe Nihal Gevrek, Yavuz Öz, Janset Yener, Harun Utku Aksoy, Hasan Can Helvacı, Ahmet Genç for their friendship. I would also thank all my friends and the members of the faculty in Chemistry Department.

I would like to thank The Scientific and Technological Research Council of Turkey (TÜBİTAK) for financial support (TÜBİTAK PROJECT 114Z139) towards this research.

Finally, my deepest thanks go to my whole family for their endless love, support and encouragement throughout these years.

ABSTRACT

NOVEL BIOFUNCTIONAL POLYESTER NANOFIBERS

In recent years, nanofibers have gained much attention in different scientific fields due to their potential applications. Increased interest arise due to their promising properties such as high surface-to-volume ratio, high encapsulation efficiency, high loading capacity and physical resemblance to the 3D structure of extracellular matrix. As health applications, nanofibers can be used in drug delivery systems, wound healing materials, tissue engineering and enzyme immobilization. Nanofibers can made via electrospinning, phase separation and self-assembly. Electrospinning is widely used because of its easiness and effectiveness. Obtained nanofibers can be functionalized with 'clickable' functional groups to suit the intended goal. This thesis focused on obtaining azide containing clickable biofunctionalizable nanofibers. In this study, a novel azide containing carbonate monomer was synthesized to obtain copolymers that were used as a precursor for electrospinning. Lactide was chosen because of its biodegradability and good mechanical properties during electrospinning. Azide containing carbonate monomer was used for functionalization of the nanofibers. Initially, efficient functionalization of nanofibers was probed using a dibenzocyclooctyne (DIBO) containing a fluorescent dye. It was deduced that the extent of functionalization of nanofibers could be tuned by amount of azide groups in the copolymers. DIBO-containing biotin was attached to the azide containing nanofibers via azide-alkyne click chemistry. Thereafter, extravidin was immobilized onto biotin functionalized nanofibers due to the high affinity of extravidin for biotin. Importantly, metal or metal-based complexes weren't used in this work for neither polymerization nor functionalization because of the potential toxicity of metals to the cells.

ÖZET

YENİ BİOFONKSİYONEL POLİESTER NANOFİBERLER

Nanofiberler son zamanlarda potensiyol uygulama alanlarından dolayı birçok bilimsel çalışma alanından ilgi görmüştür. Nanofiberlere artan bu ilginin sebebi, sundukları sayısız avantajlardır. Yüksek yüzey alanı hacim oranı, yüksek kapsülleme verimliliği, yüksek yükleme kapasitesi, fiziksel biçim olacak hücre dışı matrise benzeme; fiberlerin genel özelliklerindendir. Nanofiberlerin birçok alanda, sayısız uygulamaları vardır. Örneğin sağlık alanındaki uygulamalarına değinecek olursak; nanofiberler ilaç taşıma sistemlerinde, yara iyileştirme tedavilerinde, doku mühendisliğinde ve enzim sabitlemede kullanılabilir. Nanofiber yapma yöntemlerinden bazıları; elektrospinning, faz ayrılması ve kendiliğinde kurulmadır. Elektrospinning kolay ve verimli bir yöntem olduğu için genellikle tercih edilir. Elde edilen nanofiberler, klik reaksiyonları ile amaçlandığı şekilde fonksiyonelleştirilebilir. Bu tez, azit fonksiyonel grubu içeren klik reaksiyonu verebilecek nanofiberler üretip; bu fiberleri biyomoleküllerle fonksiyonelleştirmeye odaklanmıştır. Bu çalışmada, azit grubu içeren karbonat monomeri kopolimer yapmak için sentezlenmiştir ve bu kopolimerden lifler üretilmiştir. Laktit monomerinin seçilmesinin sebebi, biyobozunur olması ve elektrospin sırasında iyi mekanik özelliklere sahip olmasıdır. Azit içeren karbonat monomerinin kullanılmasının sebebi, elde edilecek fiberlerin klik reaksiyonu yapabilmesini amaçlamaktır. Öncelikle; nanofiberlerin verimli fonksiyonelleştirilmesi, dibenzosiklooktin (DIBO) grubu içeren floresan boya ile araştırılmıştır. Daha sonra nanofiberler, kopolimer üzerinde azit miktarları değiştirilerek ayarlanabilir. Nanofiberlerin biofonksiyonelleştirilmesi amacıyla; dibenzosiklooktin (DIBO) grubu içeren biyotin vitamini, azit-alkin klik reaksiyonu ile nanofiberlerin üzerine bağlanmıştır. Daha sonra, ekstravidinin biotine bağlanma eğilimi kullanilarak, biotin içeren fiberler ile ekstravidin sabitlenmiştir. Önemli olarak; bu projede, polimerizasyon yada klik reaksiyonu için metal veya metal kompleksi kullanılmamıştır. Çünkü, metaller hücreler için zararlıdır.

TABLE OF CONTENTS

LIST OF FIGURES

LIST OF TABLES

LIST OF ACRONYMS / ABBREVIATIONS

Bis-mPA	2,2-Bis(hydroxymethyl)propionic Acid
$CDCl_3$	Deuterated Chloroform
CH_2Cl_2	Dichloromethane
DBU	1,8-Diazabicycloundec-7-ene
DCC	N,N'-Dicyclohexylcarbodiimide
DCU	N,N'-Dicyclohexylurea
DIBO	4-Dibenzocyclooctynol
DMAP	4-Dimethylaminopyridine
DMF	Dimethylformamide
DMSO	Dimethyl Sulfoxide
EtOAc	Ethyl Acetate
FTIR	Fourier Transform Infrared Spectroscopy
GPC	Gel Permeation Chromatography
KOH	Potassium Hydroxide
LDA	Lithium Diisopropylamide
$NaHCO_3$	Sodium Bicarbonate
NaN_3	Sodium Azide
Na_2SO_4	Sodium Sulfate
PCL	Polycaprolactone

PDI	Polydispersity Index
PEG	Polyethylene Glycol
PHB	Polyhydroxybutyrate
PHBV	Poly(3-hydroxybutyrate-*co*-3-hydroxyvalerate)
PLA	Polylactide
PPY	Polypyyrole
pTsOH	p-Toluenesulfonic Acid
ROP	Ring Opening Polymerization
SEM	Scanning Electron Microscopy
THF	Tetrahydrofuran
TLC	Thin Layer Chromatography
TRITC	Tetramethyl Rhodamine
TU	1-(3,5-bis(trifluoromethyl)-phenyl)-3-cyclohexyl-2-thiou

1. INTRODUCTION

1.1. Nanofibers

Nanofibers are fibers that have diameter less than 1000 nm. In recent years, nanofibers have gained much attention from different fields. According to the Business Communication Company Research, nanofibers are one of the fastest growing component of the nanotechnology. In 2017, the market value of nanofibers are expected to be four times higher than the value in 2012 that was $151.5 million [2]. This is due to advantageous properties of nanofibers such as their extremely high surface-volume ratio, high encapsulation efficiency, tunable porosity etc.

Nanofibers are used in the area of building and construction as solar panels, thermal insulation, sound insulation; environment as air filtration, liquid filtration, photocatalyst, noise absorption, gas sensors; electronics as hard disk drives, optoelectronic devices, piezoelectric devices; energy as lithium batteries, fuel cells, solar cells; defense as warfare protection, bulletproof uniforms, anti-counterfeiting devices; consumer as food packaging, technical textile, personal care; automotive as batteries, filters, sound absorption and in health in wound dressing, tissue engineering, drug delivery systems, barrier garments, respirators etc [3].

1.1.1. Properties of Nanofibers

Nanofibers have high surface to volume ratio that improves their performance in many different areas such as sensor applications. In this area, high surface to volume ratio is a

desirable property since a large area can absorb more analyte and change the response of sensors rapidly and significantly [4]. Moreover, they have also tunable porosity that makes them a dynamic system. Unlike rigid structures, the properties of pores can be changed according to the intended aim. Nanofibers have adjustable biodegradation rate that means the time of degradation can be engineered to be proportional with the time needed for therapy. They physically resemble the structure of extra-cellular matrix, thus giving opportunity to cells to live and perform their regular functions. They also promote cell adhesion, proliferation and spreading. Moreover, they have better cell attachment, high encapsulation efficiency because of their high surface to volume ratio. The fiber morphology and scaffold composition can be changed according to the desired goal. Tunable porosity allows cell migration and transportation of metabolic waste and nutrient [3, 5].

1.1.2. Synthesis of Nanofibers

Nanofibers can be produced using techniques such as phase separation, self-assembly, template synthesis, drawing, electrospinning etc [6]. However, most of them have drawbacks such as consumption of time, energy and money, ending up with non-uniform fibers, forcing the polymer solution in very harsh conditions thus causing deformations etc [6]. Among these, electrospinning is the simplest and most effective way for obtaining uniform nanofibers (Figure 1.1). Nanofibers morphology can be manipulated through changing various parameters during electrospinnig. Electrospinning can be conducted with melt polymer or polymer in solution.

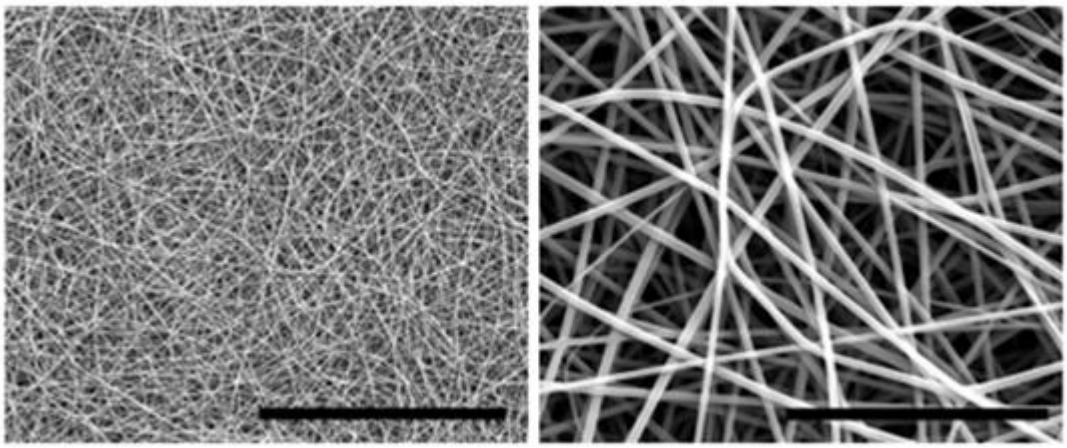

Figure 1.1. SEM images of uniform nanofibers produced using electrospinning under different magnifications [7] (Scale bars are 40 μm and 5 μm, respectively).

1.1.3. Application of Nanofibers

Nanofibers can be used in many areas such as environment, electronics, energy, defense, automotive, consumer, building, health and so on. Nanofibers for health purposes can be obtained from biodegradable polymers. Various additives can be incorporated into the fiber and that brings aimed functionality. Size, morphology and structure of nanofibers can be manipulated. Therefore, nanofibers can be optimized according to the intended aim. Nanofibers can be used in tissue engineering, drug delivery systems, wound dressing, medical prostheses and enzyme immobilization process as health applications.

Nanofibers can be used in tissue engineering [3, 4]. Nanofibers spun from biopolymers can be used a substrate for cells to grow and perform their daily functions. It is possible to design nanofibers that are suitable to implant by various types of cells. Moreover, nanofibers support proliferation of cells and facilitate tissue replacement. Nanofibers can be used in drug delivery systems because of their high surface-to-volume ratio, high encapsulation efficiency, high loading capacity, ease of operation and so on [3, 4]. They can be used as a drug carrier or bioactive material. Moreover, pharmaceutical ingredients can be put into the

nanofibers. Wound dressing is another health application of nanofibers that supports wound healing process. It is possible to incorporate drug or antibacterial compound into the nanofibers when they are used on wounds. The rate of drug release in dressing materials can be controlled using size or composition of nanofibers. Nanofibers can be used for preparing medical prostheses [8]. Size, morphology and structure of nanofibers can be controlled and optimized according to the intended aim. Moreover, nanofibers can be used in enzyme immobilization process in order to hold enzyme in its place throughout a reaction and separated easily from the products after the reaction. This type of immobilization often gives resistance to enzymes to the changes in pH or temperature etc [3, 4].

1.2. Electrospinning

Electrospinning is a simple technique for generating uniform polymeric nanofibers. It uses electrical charge to make nanofibers from a polymer containing solution. The process does not require any harsh conditions and fibers can be obtained rapidly thus making it a very useful technique for obtaining nanofibers.

Electrospinning set up consists of three components: High voltage power supply, metal collector and a needle. One electrode is brought in contact with the polymer solution and the other electrode is attached to a metal collector screen. After that, high voltage is applied and electrical field is generated between metal collector and the tip of syringe. When high voltage is applied, the solution in the syringe is charged, thus generating a charge on the surface of the solution that is held by its surface tension. After a while, electrostatic repulsions between the charges overcome the surface tension forces. The droplet of solution is stretched and emerges from the surface. This point is referred as Taylor Cone. Upon further increasing the electrical field more, the charged fluid jet is ejected from the tip of the Taylor Cone and elongated during the flight and deposited on the metal collector. During the flight, solvent evaporates and fibers are deposited on the collector [6] (Figure 1.2).

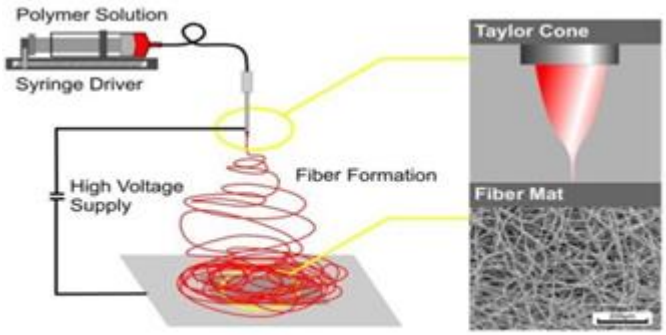

Figure 1.2. Schematic representation of electrospinning [6].

There are some electrospinning parameters that can be changed to obtain the desired nanofiber morphology: Solution parameters, operation parameters and ambient parameters. Solution parameters are the concentration of the polymer solution, molecular weight, viscosity, surface tension, conductivity as solution parameters. Operation parameters are voltage, flow rate, collectors, distance between the collector and the tip of syringe .Ambient parameters are humidity, temperature and so on [9]. Effect of some of these will be explained in detail.

1.2.1. Parameters of Electrospinning

1.2.1.1. Solution Parameters. Concentration of the polymer solution is a very crucial parameter for electrospinning. If concentration is very low, electrospraying may occur instead of electrospinning because of the low viscosity and high surface tension of the polymer solution [10]. When the concentration is too high, both beads and fibers can be formed [11]. Only when the concentration is suitable, uniform nanofibers are formed [12]. Interestingly in one case when the concentration was very high, helix microribbons are formed [13] (Figure 1.3).

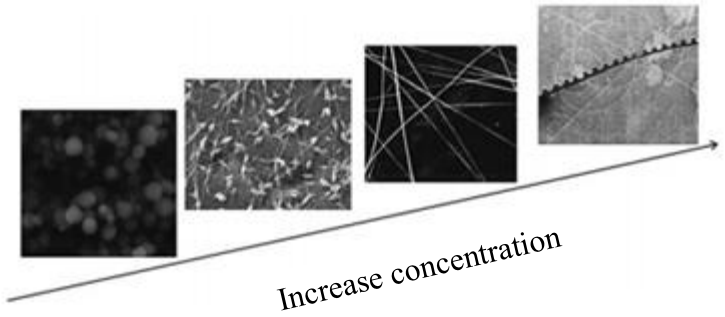

Figure 1.3. SEM images of nanofibers from low concentration to high concentration [13].

1.2.1.2. Operation Parameters. During the electrospinning process, voltage is a very crucial factor because applied voltage must be higher than the threshold voltage for the solutions to erupt from the Taylor cone to obtain a liquid charged jet.

However, voltage is a controversial issue in electrospinning. For example, Reneker and co-workers demonstrated that there is not very much effect of the voltage on the fiber diameter [14]. Some researchers said that higher voltage forms larger diameter fiber [15]. Several groups demonstrated that high voltage can increase electrostatic force on the jet liquid, causing the narrowing of fiber diameter [16].

Sanyal and co-workers demonstrated that higher voltage favors the bead-free fiber formation. Polymer solution was subjected to undergo electrospinning under different voltages such as 5.5 kV, 8 kV and 11kV. With 11 kV voltage, they obtained bead-free uniform fibers. Moreover, higher voltage favored to narrow the fiber diameter distribution and decreased the fiber diameter [17] (Figure 1.4).

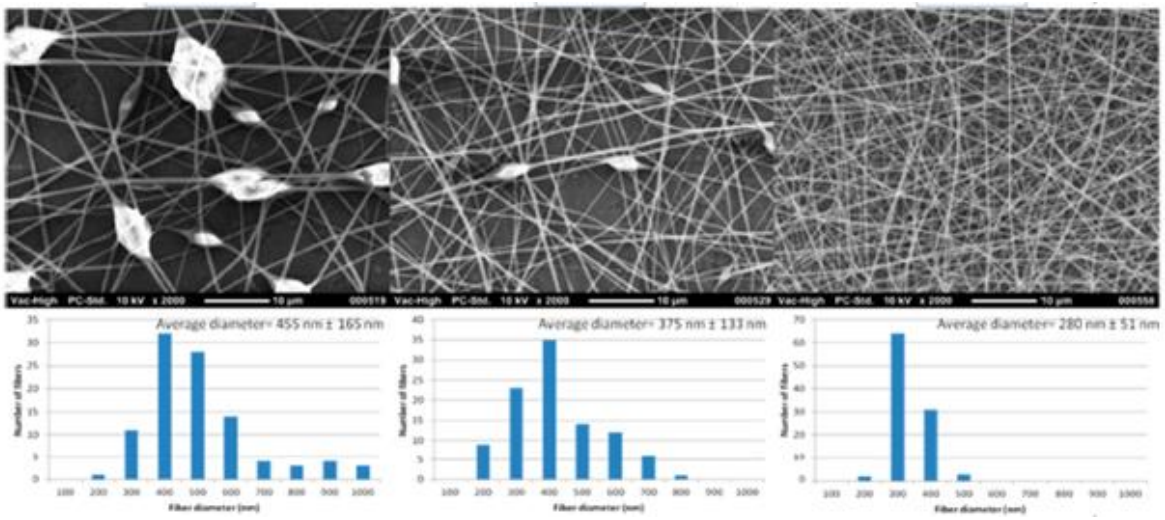

Figure 1.4. SEM images of nanofibers under different voltages: 5,5 kV, 8 kV and 11 kV from left to right [17].

Flow rate is an important parameter for electrospinning that controls uniformity of fiber. Generally, low flow rate is recommended to give the solution enough time for polarization. When the flow rate is very high, beaded fibers are formed instead of smooth, thin and uniform fibers. For example, Sanyal and co-workers recently demonstrated that fiber diameter was getting higher when the flow rate was higher. Moreover, beaded fiber structure was obtained with high flow rate [17] (Figure 1.5).

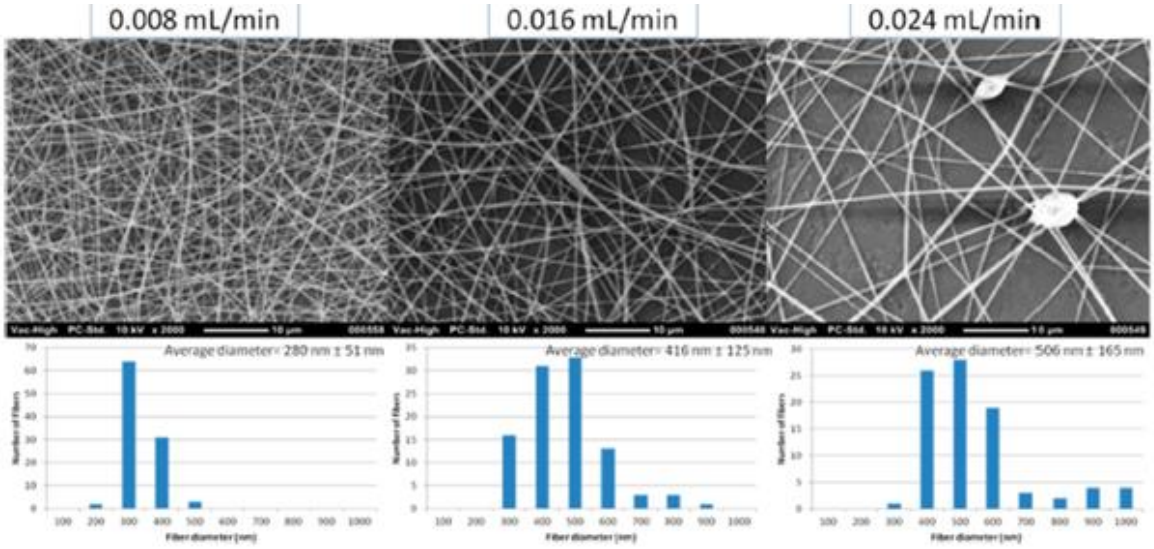

Figure 1.5. SEM images of nanofibers under different flow rates [17].

The distance between the collector and tip of the syringe affects the fiber morphology and diameters [18]. Briefly, if the distance between the collector and tip of syringe is very short, solution does not have enough time to evaporate before depositing on the collector, and thus the fibers cannot solidify. If the distance between the collector and tip of syringe is very long, then beads may form. Therefore, an optimum distance between the collector and tip of syringe needs to be established to obtain smooth, uniform, bead-free nanofibers. For example, Sanyal and co-workers demonstrated the effects of distance on fiber morphology (Figure 1.6). They electrospun polymer solution with different distances: 5 cm, 10 cm and 20 cm. Beaded thick nanofibers were obtained with 5 cm distance between tip of syringe and collector. Thinner fibers were obtained with 10 cm and polydispersity of nanofibers also decreased. Moreover, thinnest nanofibers were obtained with 20 cm distance [17]. Yuan and co-workers obtained nanofibers with 438 nm as an average diameter with 10 cm distance and 368 nm with 15 cm [9] (Figure 1.7).

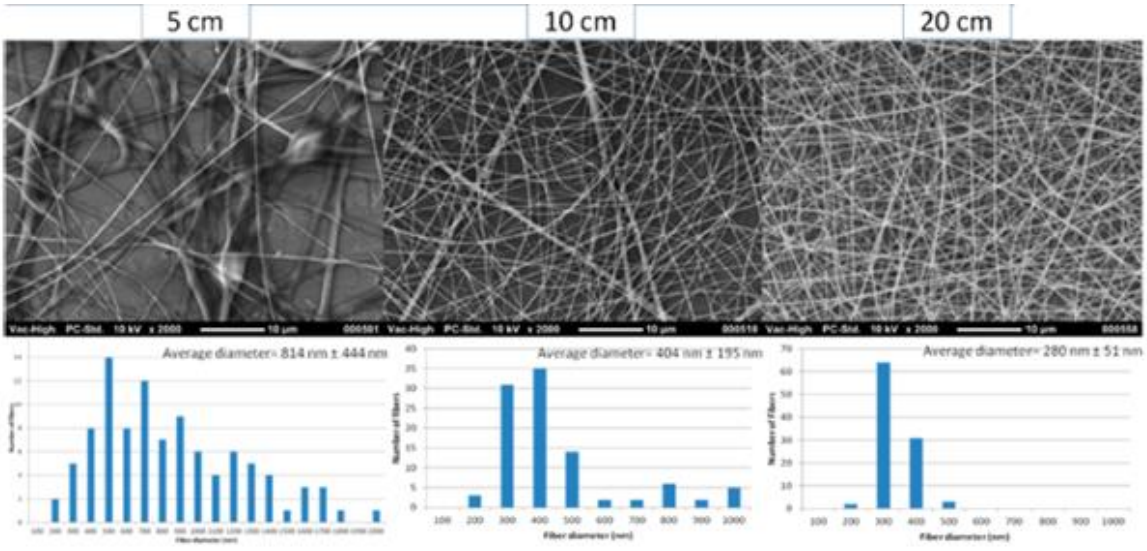

Figure 1.6. SEM images of nanofibers with different distance between collector and tip of syringe [17].

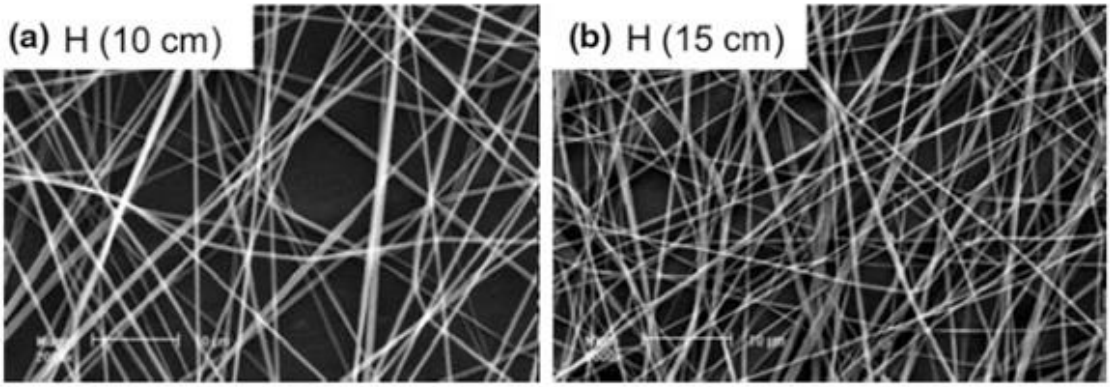

Figure 1.7. SEM images of nanofibers with different distance between collector and tip of syringe: The diameter of A: 438 nm and the diameter of B: 368 nm [9].

1.3. Biodegradable Polymers

Biodegradable polymers are polymers that decompose after its planned aim to give natural products such as water, salts and gases. Biodegradable polymers are either naturally found or made synthetically. Fibrin, gelatin and collagen are examples of natural biodegradable polymers, whereas polycaprolactone (PCL), polylactide (PLA) and polyglycolide (PGA) are examples of synthetic biodegradable polymers (Figure 1.8). They mainly include ester, amide groups on their chains that give them chemical functionality. Ring opening polymerization [19], condensation reactions [20], metal-catalyzed polymerizations are general ways to synthesize them.

Biodegradable polymers should be stable during their particular applications, whereas they should decompose easily after their intended purpose. Degradation time depends on parameters such as molecular weight, hydrophobicity and crystallinity [21].

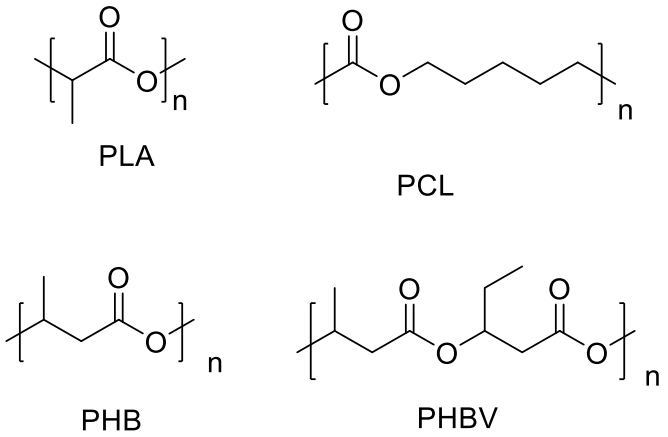

Figure 1.8. Some examples of biodegradable polymers [22].

Biodegradable polymers have received great interest and attention from many areas such as clothing, biomedical, agriculture, packaging, drug delivery systems etc. In medicinal

area, they are mostly used in tissue engineering and drug delivery systems (Table 1.1). For being a promising candidate for drug delivery system, a polymer must have these properties: polymer itself and its natural by products must be nontoxic, byproducts must be totally eliminated from the body, the time of degradation of polymer must be proportional with the time needed for therapy etc [33]. Biodegradable polymers have many uses in biomedical area due to their biodegradability and biocompatibility. They are used in tissue engineering, gene therapy, regenerative medicine. For example, many implants, bone substitution and fixing materials, dental materials are made from biodegradable polymers. These materials can be used as scaffolds, for example, muscle tissue of a rat can grow on a polylactide/polycaprolactone scaffold [34].

Table 1.1. Summary of different polymers' applications, advantages, disadvantages, degradation rate constant and structure [1].

Polymer	Applications	Advantages	Disadvantages	λ, Degradation Rate Constant (s^{-1})	Structure
Polyphosphazenes	Tissue Engineering; Vaccine Adjuvant	Synthetic Flexibility; Controllable Mechanical Properties	Complex Synthesis	$4.5 \times 10^{-2} - 1.4 \times 10^{-7}$ (refs. 13 and 776)	
Polyanhydrides	Drug Delivery; Tissue Engineering	Significant Monomer Flexibility; Controllable Degradation Rates	Low-molecular Weights; Weak Mechanical Properties	$1.9 \times 10^{-3} - 9.4 \times 10^{-9}$ (refs. 17 and 777)	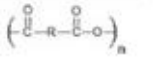
Polyacetals	Drug Delivery	Mild pH Degradation Products; pH Sensitive Degradation	Low Molecular Weights; Complex Synthesis	6.4×10^{-5} (ref. 17)	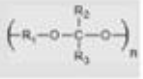
Poly(ortho esters)	Drug Delivery	Controllable Degradation Rates; pH Sensitive Degradation	Weak Mechanical Properties; Complex Synthesis	4.8×10^{-5} (ref. 17)	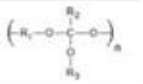
Polyphosphoesters	Drug Delivery; Tissue Engineering	Biomolecule Compatibility; Highly Biocompatible Degradation Products	Complex Synthesis	1.4×10^{-6} (refs. 778 and 779)	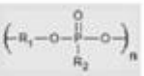
Polycaprolactone	Tissue Engineering	Highly Processable; Many Commercial Vendors Available	Limited Degradation	3.5×10^{-8} (ref. 27)	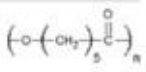
Polyurethanes	Prostheses; Tissue Engineering	Mechanically Strong; Handle Physical Stresses Well	Limited Degradation; Require Copolymerization with Other Polymers	8.3×10^{-9} (ref. 780)	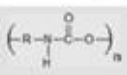
Polylactide	Tissue Engineering; Drug Delivery	Highly Processable; Many Commercial Vendors Available	Limited Degradation; Highly Acidic Degradation Products	6.6×10^{-9} (ref. 17)	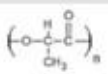
Polycarbonates	Drug Delivery; Tissue Engineering; Fixators	Chemistry-Dependent Mechanical Properties; Surface Eroding	Limited Degradation; Require Copolymerization with Other Polymers	4.1×10^{-10} (ref. 285)	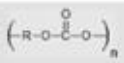

1.3.1. Synthesis Via Ring Opening Polymerization

Biodegradable polymers can be synthesized via ring opening polymerization (ROP) and condensation reactions. Usually a better control in polymerization and uniformity in chain lengths is obtained using ROP. Commonly utilized types of ring opening polymerization are anionic ring opening polymerization and cationic ring opening polymerization. There are two types of ring opening polymerizations in terms of types of catalysts which are metal-catalyzed ring opening polymerizations and organocatalyzed ring opening polymerizations.

1.3.1.1. Anionic Ring Opening Polymerization. Anionic ring opening polymerization is a specific type of polymerization that utilizes a nucleophilic reagent as an initiator. Monomers that have polarized functional groups can undergo anionic ring opening polymerizations. In a polarized functional group, there is one electron deficient atom in structure because of the existence of another adjacent atom that is highly electronegative. Polymerization starts with the attack of the nucleophile to the electron deficient atom in the ring producing an intermediate that will behave as a nucleophile. Ideally, process will continue until most monomer is consumed [23] (Figure 1.9).

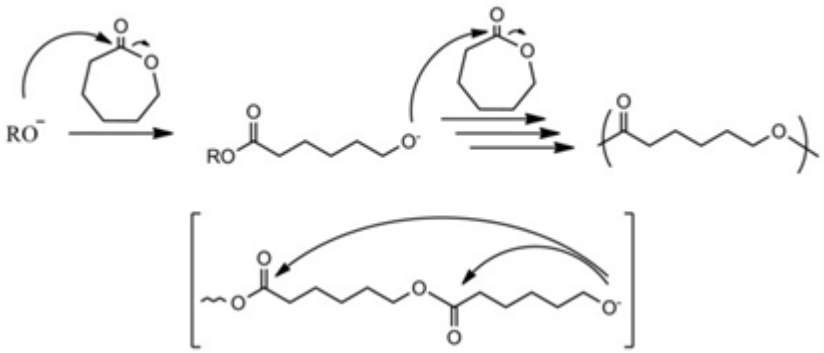

Figure 1.9. Anionic ring opening polymerization of ε-caprolactone [24].

1.3.1.2. Cationic Ring Opening Polymerization. Cationic ring opening polymerization is a specific type of polymerization that has a cationic intermediate and initiator (Figure 1.10). Amines, ethers, lactones are monomers that can undergo cationic ring opening polymerization [25]. The mechanism of the polymerization can go through S_N1 or S_N2 propagation step and chain growth step [25]. Depending on the stability of cationic species, the mechanism is determined.

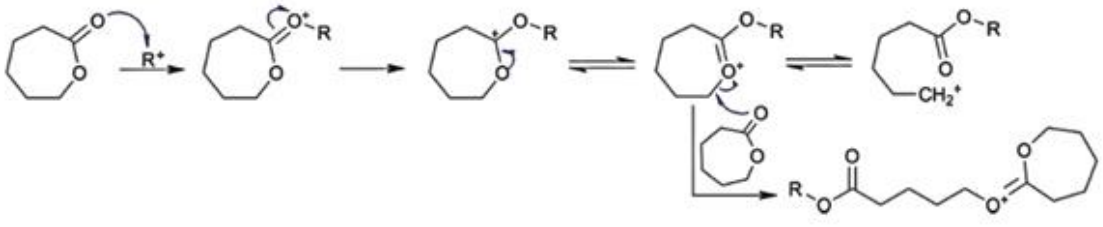

Figure 1.10. Mechanism of initiation step of cationic ring opening polymerization of ε-caprolactone [26].

1.3.1.3. Metal-catalyzed Ring Opening Polymerizations. Metals can be used in ring opening polymerizations as catalysts that are generally organometallic complexes. These complexes are generally based on transition metals and they show good performance in ring opening polymerizations. For example, Wang and co-workers presented a kinetic analysis study of the metal-catalyzed ring opening polymerization of cyclic ester with Tin(II) octoate [27] (Figure 1.11). However, metals are toxic for cells; therefore, they may pose problems especially in vivo studies. Luximon and co-workers studied polymerization of ε-caprolactone by using lithium diisopropylamide (LDA) as a catalyst. Reaction proceeded through anionic ring opening polymerization. Obtained polymer was biodegradable but was not suitable for scaffolds for vivo studies because of toxicity of metals towards cells [28].

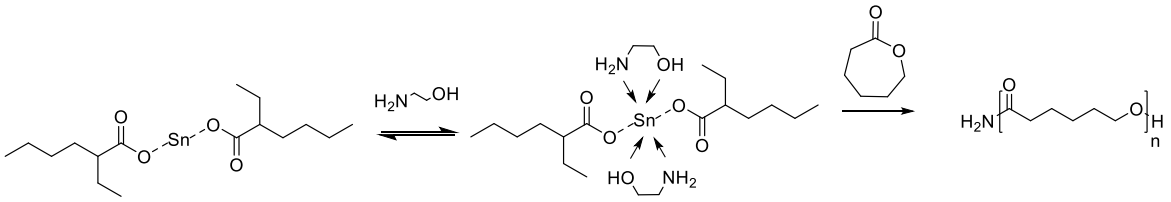

Figure 1.11. Metal catalyzed ring opening polymerization of ε-caprolactone [27].

1.3.1.4.Organo-catalyzed Ring Opening Polymerizations. In organo-catalyzed ring opening polymerizations, organic complexes are used as catalysts rather than metal catalysts that are known to be toxic for cells. In 2001, Nederberg and co-workers made the first approach to the organo-catalyzed ring opening polymerization of the lactide monomer. They used polypyrrole (PPY) and 4-dimethylaminopyridine (DMAP) as catalysts and ethanol as initiator [29]. Pyridine based complexes, phosphine based complexes, N-heterocyclic carbenes are used as a catalyst in ring opening polymerizations.

In 2006, Dove and co-workers polymerized caprolactone by using pyrenebutanol as an initiator; 1,8-Diazabicycloundec-7-ene (DBU) and 1-(3,5-bis(trifluoromethyl)-phenyl)-3-cyclohexyl-2-thiourea (TU) as catalysts (Figure 1.12). They studied polymerization with different types of initiators and catalysts [30]. Organocatalyzed polymerizations yield polymers that can be used for vivo studies because of their nontoxicity to cells.

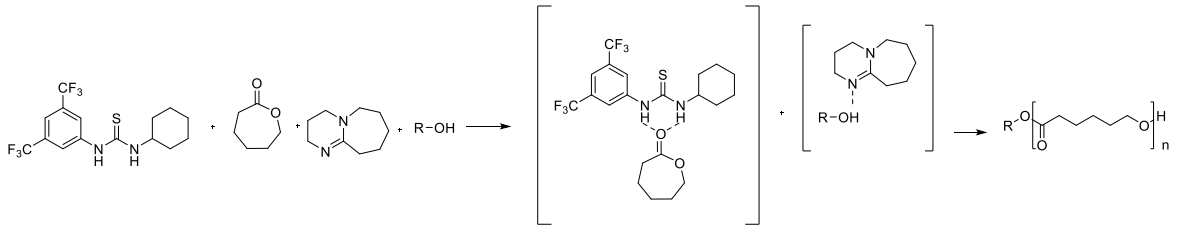

Figure 1.12. Organocatalyzed ring opening polymerization of caprolactone.

1.3.2. Condensation Reactions

Some biodegradable polymers such as polylactide can be synthesized via condensation reactions. Beginning with the lactic acid, one can follow two ways to obtain polylactide. Firstly, lactide can be synthesized from lactic acid via condensation reactions and then polylactide can be synthesized via ring opening polymerization from lactide

monomer. Secondly, only condensation reactions can be used to synthesize polylactide from lactic acid [31]. However, water must be eliminated from the media to push the reaction forward.

Maharana and co-workers polymerized lactic acid through condensation polymerization reaction. They obtained polylactide as a product and water as a by-product. Water must be eliminated from the media to push the reaction forward. Thus, they tried to optimize equilibrium between lactic acid, water and polylactide by using multifunctional branching agent or an organic solvent [32] (Figure 1.13).

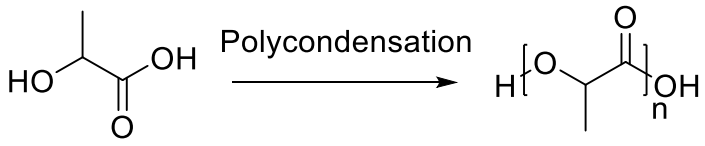

Figure 1.13. Polycondensation of lactic acid.

1.4. Click Chemistry

Click reactions are reactions that undergo transformations with very high yields. In general, they are easy to perform, selective, and produce byproducts that can be removed very easily without chromatography. The term ‘click chemistry’ was firstly introduced by Sharpless in 1998 and it was described in detail by Sharpless, Kolb and Finn in 2001 [35]. Click reactions are very powerful tool in synthesis because of above mentioned characteristics. To date, click reactions have been used to synthesize dendrimers, hydrogels, block copolymers and other polymeric materials. Click reactions that are frequently used are azide-alkyne cycloaddition, thiol-ene radical addition, Michael addition and the Diels-Alder

reactions. In my project, I utilize the azide-alkyde cycloaddition reaction described below in detail.

1.4.1. Azide Alkyne Cycloaddition

Azide-alkyne cycloaddition was introduced by Rolf Huisgen [36]. Therefore, this reaction is often referred as a Huisgen 1,3 dipolar cycloaddition. It involves a reaction between an alkyne dipolarophile and a 1,3 dipole like azide to obtain a five-membered ring. Azide alkyne cycloaddition reaction is an ideal click reaction except that it produces a mixture of 1,4 disubstituted triazole and 1,5 disubstituted triazoles (Figure 1.14).

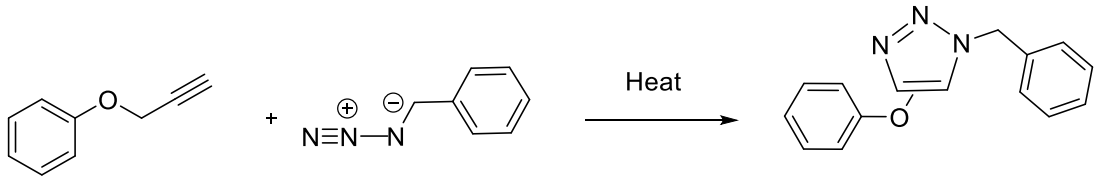

Figure 1.14. General scheme of click reaction between an azide and a terminal alkyne [37].

In recent years, two main types of azide alkyne cycloaddition have emerged, which are Cu(I) catalyzed [38] and strain-promoted [39]. These cycloadditions proceed with high efficiency at milder temperatures.

1.4.1.1. Cu (I) Catalyzed Azide-alkyne Cycloaddition. In 2003, Sharpless and co-workers demonstrated the high selectivity of reaction between azide and terminal alkyne when Cu(I) catalysis was used [40]. The reaction favors to form 1,4-disubstituted 1,2,3-triazoles with very high selectivity (Figure 1.15). Moreover, this reaction is very easy to perform and involves easy purification when compared to other organic reactions. Also, it is not sensitive to water and air and there is no by-product at the end of the reaction. All of these features make this cycloaddition an ideal click reaction. Therefore, there are many applications of azide alkyne cycloaddition in drug delivery systems, organic chemistry and so on. However, there are some drawbacks such as Cu is known to be toxic for living organisms. Therefore, it may not be suitable for the cell studies because of the high toxicity if residual copper species are present in the product.

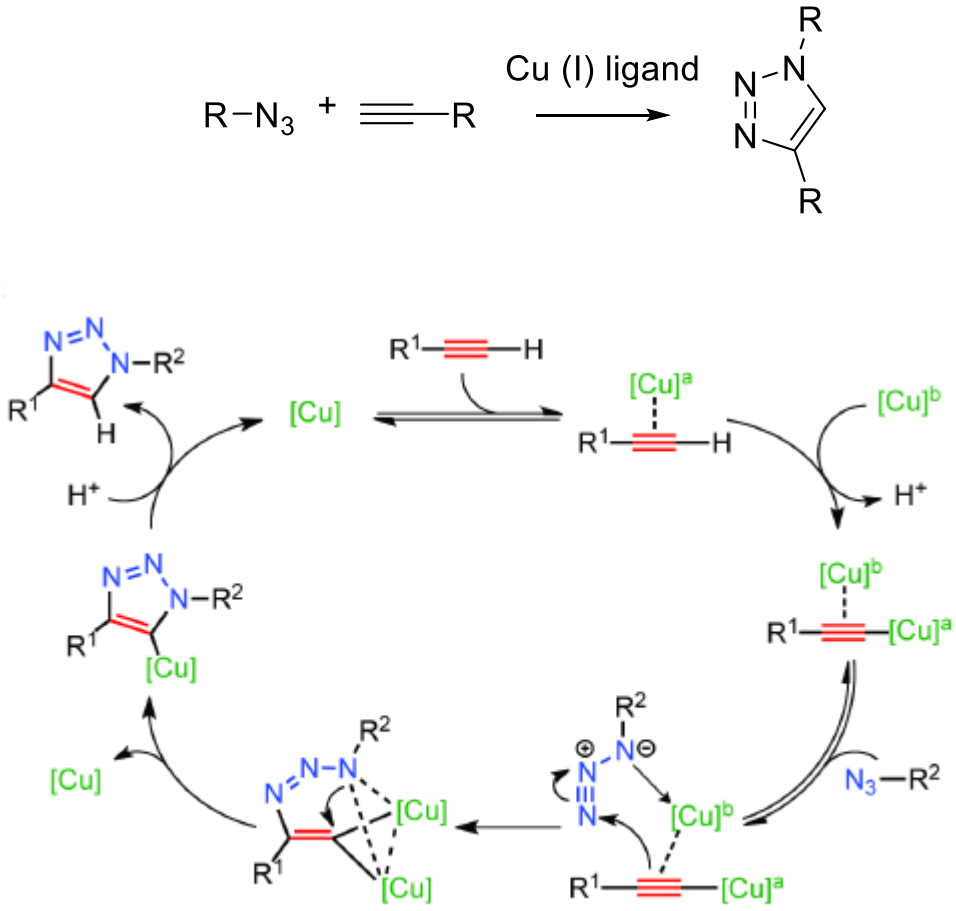

Figure 1.15. Proposed reaction mechanism of azide-alkyne cycloaddition with Cu(I) catalyst [41].

Becker and co-workers functionalized their nanofibers by using Cu(I) catalyzed azide-alkyne cycloaddition [38]. They synthesized amino acid-based polyester ureas that have clickable groups on it for biomedical applications. Clickable groups on the copolymer were azide, alkyne, alkene, ketone and tyrosine-phenol. Cu(I) catalyzed azide-alkyne cycloaddition was used for functionalization of nanofibers that contained azide and alkyne clickable group on them. Chrome 488 azide was utilized for functionalization of alkyne bearing nanofibers (Figure 1.16a) and they used alkyne-RGD-biotin for functionalization of azide bearing nanofibers. After biotin was attached via copper catalyzed azide-alkyne cycloaddition, rhodamine conjugated streptavidin was immobilized (Figure 1.16b).

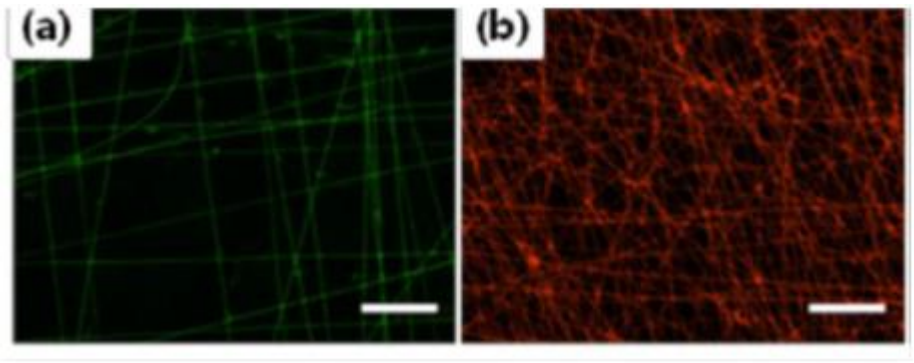

Figure 1.16. Fluorescent images of nanofibers; scale bars are 50 μm [38].

1.4.1.2. Strain-promoted Azide-alkyne Cycloadditions. In 2004, Bertozzi and co-workers disclosed a new pathway to synthesize triazole without using Cu catalysis since Cu catalyst could be toxic to cells and thus limits the application areas of using azide-alkyne cycloaddition reaction. They demonstrated a strain-promoted cycloaddition (3+2) between azides and cyclooctynes that proceeds under physiological conditions without the need for metal catalyst (Figure 1.17), with high selectivity and no toxicity to cells [39]. Therefore, this strain-promoted cycloaddition is a promising candidate especially for *in vitro* and *in vivo* studies.

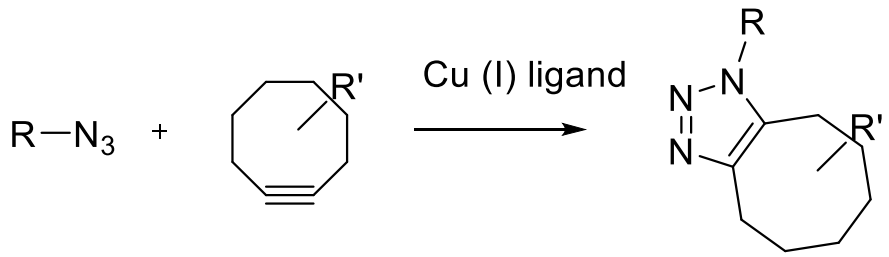

Figure 1.17. Strain-promoted (3+2) cycloaddition of azides and cyclooctynes [39].

Becker and co-workers functionalized nanofibers via strain-promoted azide-alkyne cycloaddition. They used DIBO containing polymer to obtain cycloalkyne containing nanofibers via electrospinning (Figure 1.18). After electrospinning, there were available DIBO groups on the surface of nanofibers. They demonstrated that there are available DIBO groups on the surface for functionalization via strain-promoted azide-alkyne cycloadditions. They used an azide containing fluorescent probe for click reaction. Furthermore, they also used azide containing gold nanoparticles for fiber functionalization [42].

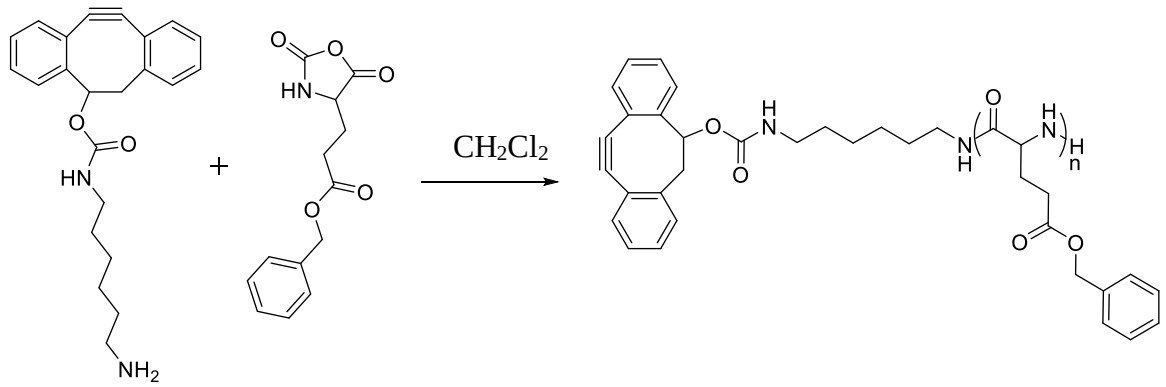

Figure 1.18. An example of synthesizing DIBO containing polymer for strain-promoted azide-alkyne cycloaddition [42].

After synthesizing DIBO containing polymer, they electrospun the polymer and they functionalized nanofibers with azide-containing fluorescent probe via strain-promoted azide-alkyne cycloaddition (Figure 1.19).

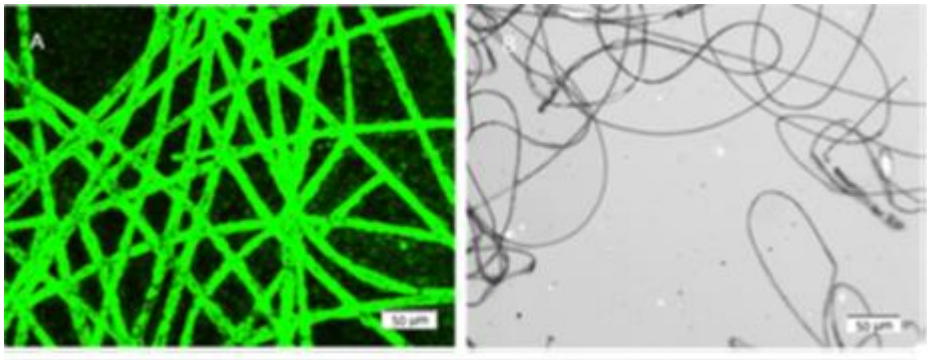

Figure 1.19. Fluorescence image of alkyne (DIBO) modified nanofibers(A) and optical image of unmodified nanofibers [42].

2. AIM OF THE STUDY

The aim of this study is to synthesize azide-containing novel reactive polyester nanofibers and functionalize them with small molecules or biomolecules (Figure 2.1).

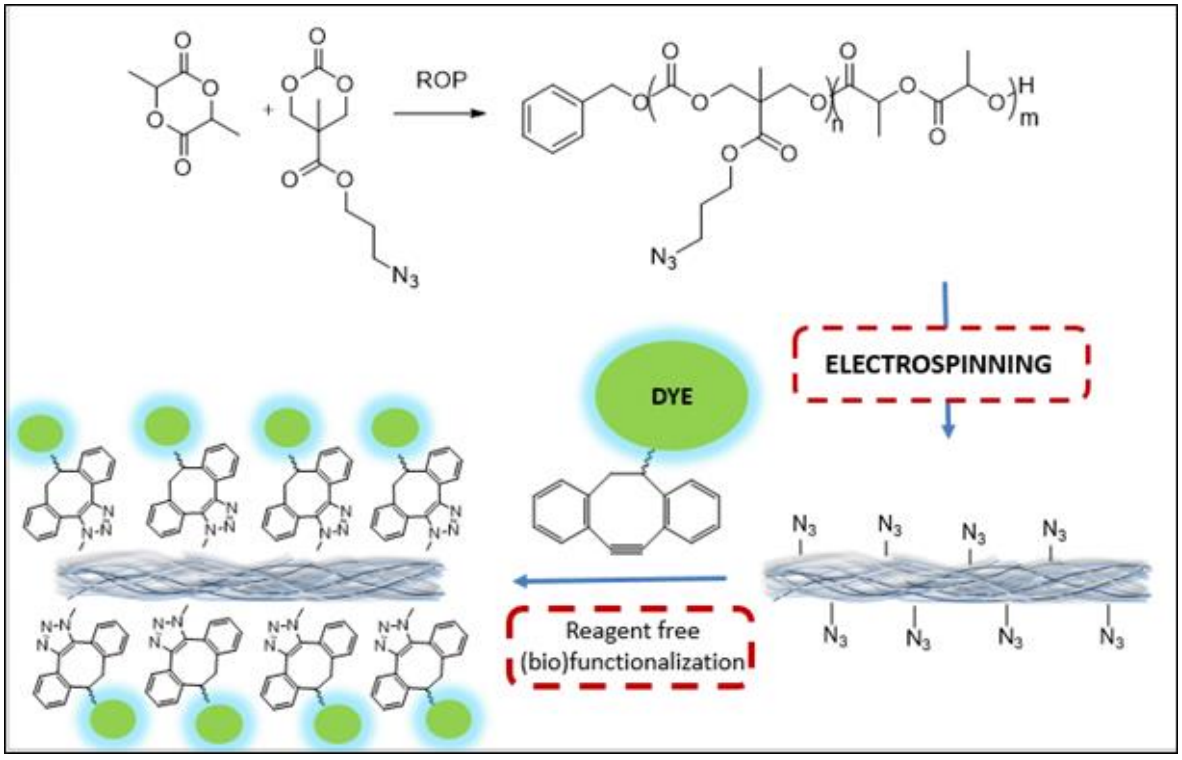

Figure 2.1. General scheme of project.

An azide-containing carbonate monomer will be synthesized for utilization in obtaining reactive copolymer. Azide-containing reactive copolymer will be electrospun to obtain uniform fibers. After obtaining nanofibers, their functionalization with fluorescent dye and ligands containing a strained alkyne group will be attempted. Tunability of nanofibers functionalization by variation of amount of azide group on copolymer will be evaluated. Finally, then nanofibers will be tested for selective protein immobilization.

3. EXPERIMENTAL

3.1. General Methods and Materials

All reagents were bought from commercial sources such as Merck, Alfa Aesar, Aldrich. Hexane, ethylacetate, dichloromethane, methanol were distilled before using. ^{1}H NMR and ^{13}C NMR spectroscopy (Varian 400 MHz), Fourier transform infrared (FTIR) spectroscopy (Perkin Elmer 1600 Series), Gel Permeation Chromatography (GPC) were used for the characterization of the compounds. The NMR spectra were recorded using a 400 MHz Varian spectrometer at 25 ^{o}C. ^{1}H NMR measurements were made at frequency of 400 MHz, and calibrated with respect to the solvent signal. The measurements were performed in deuterated chloroform ($CDCl_3$) and dimethyl sulfoxide (DMSO). The molecular weights of the polymers were estimated by GPC analysis using a Shimadzu PSS-SDV (length/ID 8x300 mm, 10 mm particle size) mixed-C column calibrated with polystyrene standards (1-150 kDa) using a refractive-index detector. Tetrahydrofuran (THF) was used as eluent at a flow rate of 1.0 mL min^{-1} at 30 ^{o}C.

3.2. Synthesis of Azide Containing Carbonate Monomer

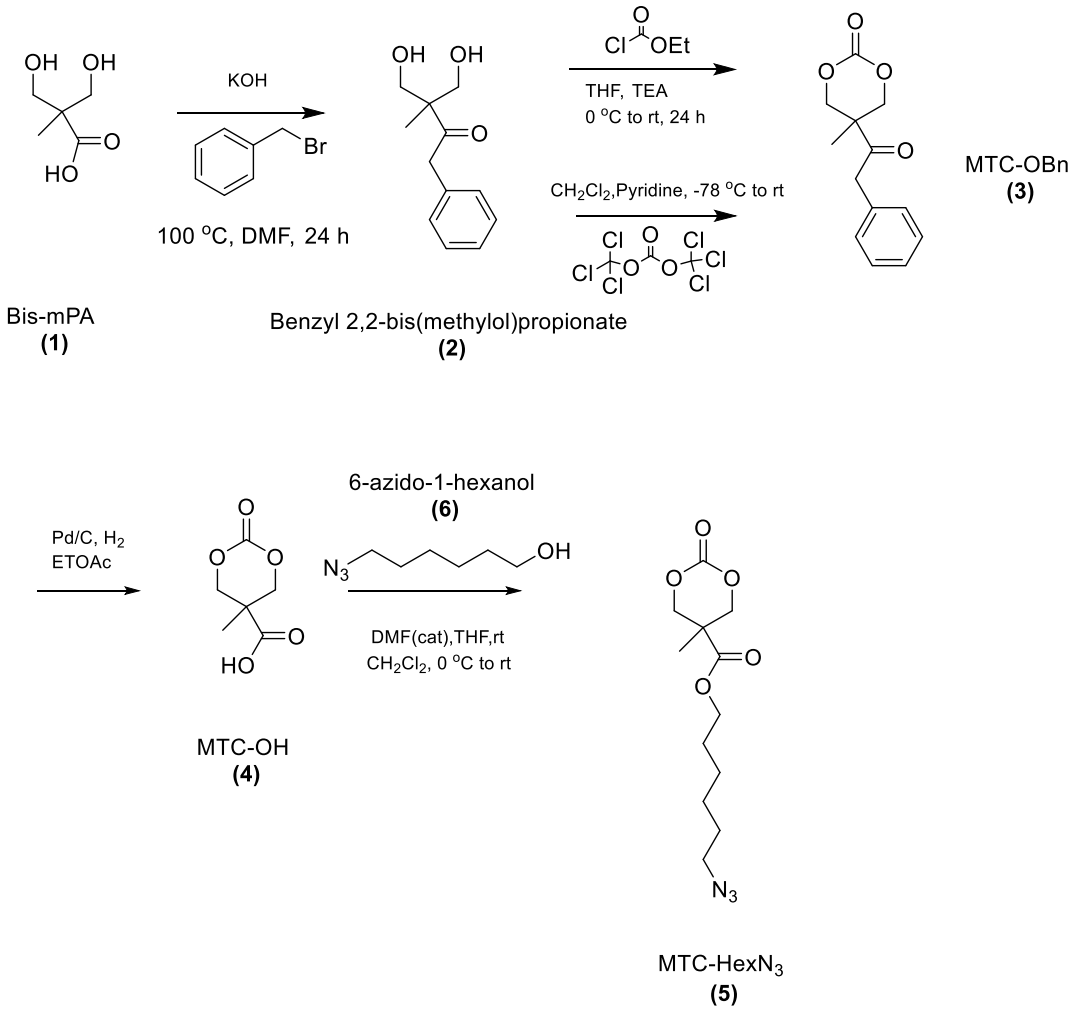

Figure 3.1. Overall scheme for synthesis of azide containing carbonate monomer **(5)**.

3.2.1. Synthesis of Benzyl 2,2-bis(methylol)propionate (2)

Benzyl 2,2-bis(methylol)propionate **(2)** was prepared according to the previously reported literature procedure previously [43]. A mixture of bis-mPA (2,2-bis(hydroxymethyl)propionic acid) (4.5 g, 0.03 mol) and KOH (2.15 g, 0.04 mol) in DMF (25 mL) was heated to 100 ^{o}C for 1 hour. After 1 hour, benzyl bromide (4.8 mL, 0.04 mol) was added to the solution and stirring was continued at 100 ^{o}C for 24 h. After 24 h, the reaction was cooled and the solvent was removed under vacuum. Then, reaction mixture was extracted with ethylacetate (30 mL), hexane (30 mL) and water (20 mL). Organic layer was retained and washed with water (2x20 mL), dried with Na_2SO_4 and the residue was concentrated in *vacuo.* A white solid was obtained and recrystallized from toluene to obtain pure product (5.1 g, 76% yield).

3.2.2. Synthesis of MTC-OBn (3)

Benzyl 2,2-bis(methylol)propionate (5.1 g, 0.023 mol) was dissolved in anhydrous THF (75 mL). Ethylchloroformate (4.37 mL, 0.046 mol) was then added and the solution was chilled to 0 ^{o}C by using ice-bath. Then, triethlyamine (9.62 mL, 0.069 mol) was added dropwise and stirring was continued for 24 h. The by-product formed during the reaction was filtered off and filtrate was concentrated in *vacuo*. A yellowish solid was obtained and purified by recrystallization from diethylether. Finally, a pure white solid was obtained (4.6 g, 80% yield). ^{1}H NMR (400 MHz, $CDCl_3$) δ 7.48 – 7.25 (m, 5H), 5.20 (s, 2H), 4.68 (d, *J* = 10.8 Hz, 2H), 4.18 (d, *J* = 10.8 Hz, 2H), 1.31 (s, 3H).

MTC-OBn can also be obtained by following another pathway [43]. Benzyl 2,2-bis(methylol)propionate (3.19 g, 0.014 mol) was dissolved in dichloromethane (40 mL) and pyridine (7.12 mL, 0.084 mol) under a nitrogen atmosphere and the solution was chilled to -78 ^{o}C by using cryostat. After a while, a solution of triphosgene (2.1 g, 0.007 mol) in DCM

was added to the cold solution dropwise over 1 h and the reaction was stirred at room temperature for 2 h. After 2 h, the reaction was finished by adding saturated NH_4Cl solution (25 mL). After that, organic layer was kept and washed with 1 M HCl solution (3x30 mL), saturated $NaHCO_3$ (30 mL), dried with Na_2SO_4, filtered and evaporated. Orange or yellowish solid was obtained and recrystallized from diethylether to give pure MTC-OBn (2.4 g, 69% yield).

3.2.3. Synthesis of MTC-OH (4)

MTC-OH **(4)** was prepared according to the previously reported literature procedure previously [44]. MTC-OBn (4.6 g, 0.018 mol), EtOAc (50 mL) and Pd/C (0.27 g, 0.0025 mol) was stirred under H_2 gas for 24 h. After 24 h, THF (50 mL) was added to the solution and the solution was filtered through THF-wetted celite using a sintered glass funnel. The filtrate was evaporated to yield a white solid (1.9 g, 65% yield). No further purification was needed. ^{1}H NMR (400 MHz, DMSO) δ 13.41 (s, 1H), 4.50 (d, *J* = 6.3, 5.4 Hz, 2H), 4.36 – 4.22 (d, 2H), 1.13 (s, 3H).

3.2.4. Synthesis of 6-azido-1-hexanol (6) and MTC-HexN_3 (5)

For the synthesis of 6-azido-1-hexanol, NaN_3 (5.85 g, 0.09 mol) was dissolved in 20 mL distilled water and 6-chloro-1-hexanol (4 mL, 0.03 mol) was added to the mixture. The reaction was stirred at 100 ^oC under reflux for 20 h. After 20 h, ethylacetate (20 mL) was added to the solution; organic layer was separated and washed with water (2x20 mL). Organic phase was collected and solvent was removed under *vacuo* to yield pure 6-azido-1-hexanol (4 g, 93% yield) **(6)**.

After synthesizing 6-azido-1-hexanol, MTC-HexN_3 **(5)** was synthesized according to the previously reported literature procedure previously [45]. MTC-OH (0.5 g, 0.003 mol) was dissolved in anydrous THF (9 mL) with three drops of DMF. Oxalylchloride (0.5 mL, 0.006 mol) was added dropwise and the reaction was stirred under N_2 for 1 h. After 1 h, volatiles were removed and a yellowish material (MTC-Cl) was obtained. MTC-Cl was dissolved in anhydrous CH_2Cl_2 (9 mL), and chilled to 0 ^oC by using an ice-bath. A solution of 6-azido-1-hexanol (0.4 g, 0.003 mol) and anhydrous pyridine (0.24 mL) in anhydrous CH_2Cl_2 (9 mL) was added dropwise. The mixture was allowed to come to room temperature and stirred for 4 h. 1 M NaCl (20 mL) was added to the mixture; organic layer was separated and washed with 1 M NaCl solution (2x20 mL). Organic phase was collected, dried with Na_2SO_4 and filtered. A yellowish liquid was obtained after solvents were evaporated under reduced pressure. **(5)**. Yield could not be calculated because pure product was not obtained.

3.3. Second Way of Synthesis of Azide Containing Carbonate Monomer

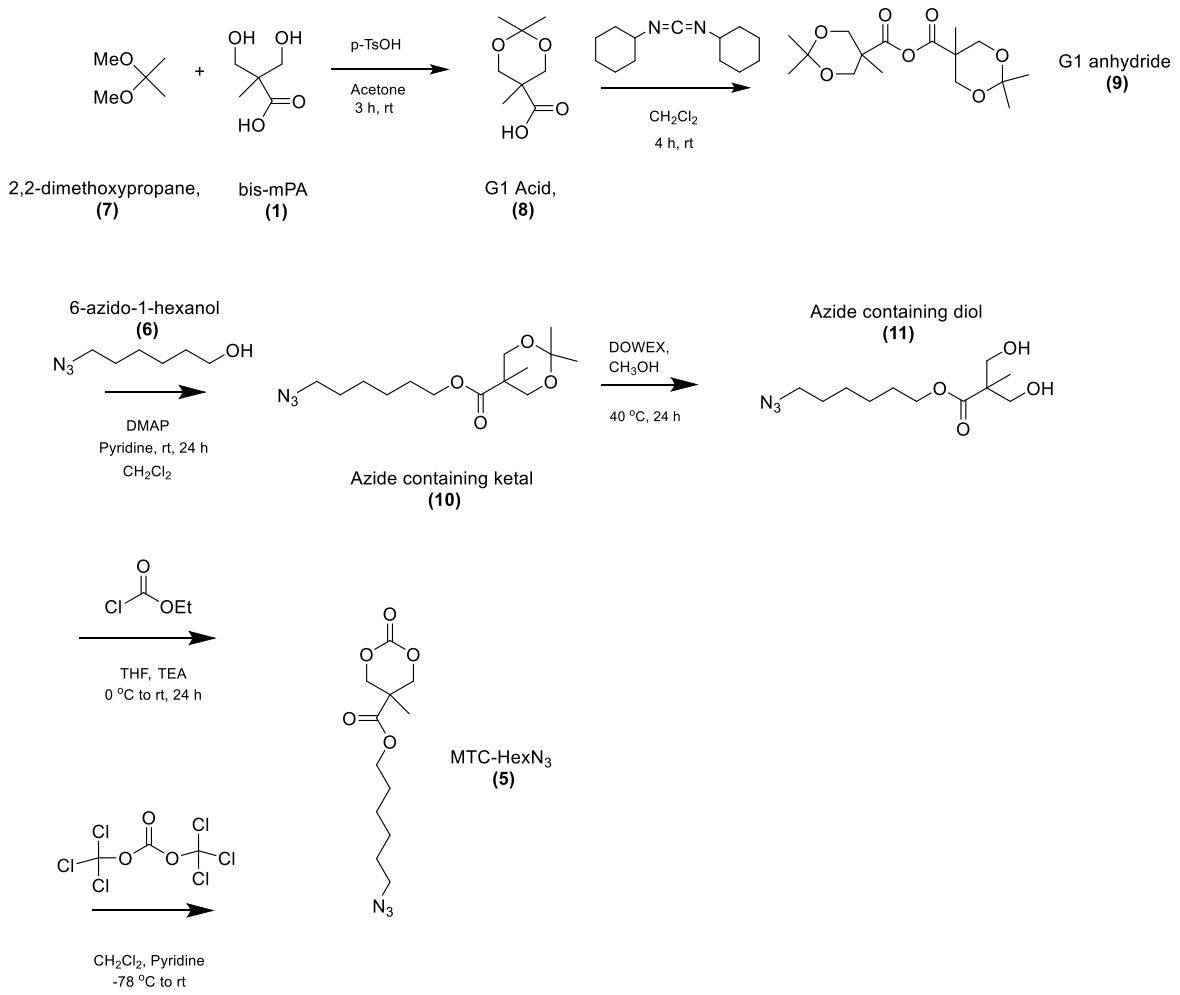

Figure 3.2. Second route for synthesizing azide containing carbonate monomer **(5)**.

3.3.1. Synthesis of G1 Acid (8)

Bis-mPA (5 g, 0.037 mol) and p-TsOH (0.35 g, 0.0018 mol) were dissolved in anhydrous acetone (20 mL) in a round bottom flask. Then, 2,2-dimethoxypropane (6.88 mL,

0.056 mol) was added. Reaction was stirred for 3 h at room temperature. After 3 h, triethylamine (0.3 mL) was added to neutralize excess p-TsOH. Volatiles were removed under vacuum and CH_2Cl_2 (20 mL) was added to the residue. Organic layer was retained and washed with water (2x20 mL), dried with Na_2SO_4 , filtered and evaporated to give G1 acid as a white solid. The resulting compound was purified by column chromatography (hexane/ethylacetate) to obtain pure compound (3.74 g, 58% yield).

3.3.2. Synthesis of G1 Anhydride (9)

G1 acid (3.74 g, 0.022 mol) was dissolved in anhydrous CH_2Cl_2 (20 mL). DCC (2.22 g, 0.011 mol) was dissolved in anhydrous CH_2Cl_2 (20 mL). DCC containing solution was added to G1 acid containing solution under N_2. Reaction mixture was stirred at room temperature for 4 h. After 4 h, formed DCU was filtered with a sintered glass funnel. CH_2Cl_2 was removed under vacuum and the residue was dissolved in cold EtOAc (40 ml). Excess DCC was filtered off with a sintered glass funnel. The filtrate was evaporated under *vacuo* to yield pure oily compound (3.1 g, 85% yield).

3.3.3. Synthesis of Azide Containing Ketal (10)

DMAP (0.28 g, 0.002 mol) was added to G1 anhydride (3.1 g, 0.009 mol) in anhydrous CH_2Cl_2 (40 mL). Then, 6-azido-1-hexanol (0.67 g, 0.0045 mol) was added to the solution. Pyridine (1 mL, 0.0135 mol) was added to the solution dropwise and the reaction mixture was stirred for 24 h. After 24 h, water (0.93 mL) was added to the reaction mixture and stirred vigorously for 3 h. After that, the solution was extracted with $NaHSO_4$, Na_2CO_3 and brine solutions. Organic phase was retained, dried with Na_2SO_4 and concentrated under *vacuo*. The resulting compound was purified by column chromatography (hexane/ethylacetate) to yield pure compound (1 g, 74% yield)

3.3.4. Synthesis of Azide Containing Diol (11)

Azide containing ketal (1 g, 0.003 mol), a spoon of previously washed DOWEX-H^+ (with methanol) and methanol (25 mL) was stirred under N_2 at 40 ^oC for 24 h. After, Dowex-H^+ was filtered off and methanol was evaporated. The resulting product was purified by column chromatography (hexane/ethylacetate) to obtain pure compound (0.6 g, 77% yield).

3.3.5. Synthesis of MTC-HexN_3 (5)

In this step, there were two paths to follow. The procedures were as mentioned page 25, 26 (procedures of synthesizing of MTC-OBn **(3)**). At least one by-product was obtained with the second way of synthesizing carbonate monomer. As mentioned before, carbonate monomer could not be obtained in pure form with neither crystallization nor column chromatography. Therefore, another short chain azide containing carbonate monomer was synthesized with the hope of purification by recrystallization (Figure 3.3)

3.4. Synthesis of Carbonate Monomer Containing Short Chain Azide

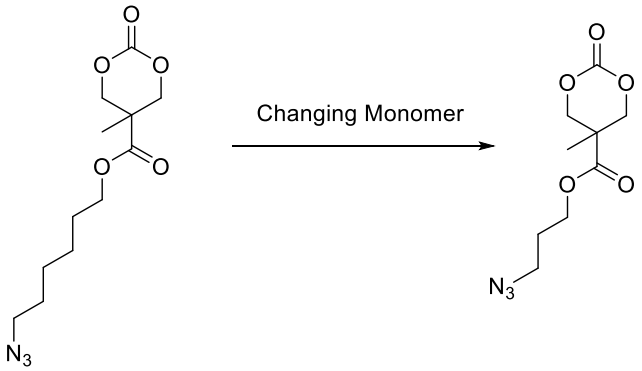

First synthesized monomer, **(5)**, MTC-HexN_3

Second synthesized monomer, **(13)**, MTC-PropN_3

Figure 3.3. Structures of carbonate monomers.

3.4.1. Synthesis of 3-azido-1-propanol (12)

For the synthesis of 3-azido-1-hexanol, NaN_3 (5.85 g, 0.09 mol) was dissolved in 20 mL distilled water and 3-bromo-1-propanol (2.7 mL, 0.03 mol) was added to the mixture. The reaction was stirred at 100 ^oC under reflux for 20 h. After 20 h, ethylacetate (20 mL) was added to the solution; organic layer was separated and washed with water (2x20 mL). Organic phase was collected and solvent was removed under *vacuo* to yield pure 3-azido-1-propanol (2.6 g, 89% yield) **(12)**. ^1H NMR was used for characterization. ^1H NMR (400 MHz, $CDCl_3$) δ 3.73 (t, J = 5.9 Hz, 2H), 3.48 – 3.37 (m, 2H), 1.86 – 1.77 (m, 2H).

3.4.2. Synthesis of MTC-PropN_3 Carbonate Monomer (13)

MTC-PropN_3 **(13)** was synthesized according to the previously reported literature procedure previously [45]. MTC-OH (0.5 g, 0.003 mol) was dissolved in anydrous THF (9 mL) with three drops of DMF. Oxalylchloride (0.5 mL, 0.006 mol) was added dropwise and the reaction was stirred under N_2 for 1 h. After 1 h, volatiles were removed and a yellowish material (MTC-Cl) was obtained. MTC-Cl was dissolved in anhydrous CH_2Cl_2 (9 mL), and chilled to 0 ^oC by using an ice-bath. A solution of 3-azido-1-propanol (0.3 g, 0.003 mol) and anhydrous pyridine (0.24 mL) in anhydrous CH_2Cl_2 (9 mL) was added dropwise. The mixture was allowed to come to room temperature and stirred for 4 h. 1 M NaCl (20 mL) was added to the mixture; organic layer was separated and washed with 1 M NaCl solution (2x20 mL). Organic phase was collected, dried with Na_2SO_4 and filtered. A yellowish liquid was obtained after solvents were evaporated under reduced pressure. **(5)**. (0.4 g, 55% yield). ^1H NMR and ^{13}C NMR were used for characterization. ^1H NMR (400 MHz, $CDCl_3$) δ 4.67 (d, *J* = 10.7 Hz, 2H), 4.29 (t, *J* = 6.2 Hz, 2H), 4.19 (d, *J* = 10.7 Hz, 2H), 3.39 (t, *J* = 6.5 Hz, 2H), 1.93 (m, *J* = 6.3 Hz, 2H), 1.31 (s, 3H). ^{13}C NMR (100 MHz, $CDCl_3$) δ 170.8, 147.1, 77.1, 76.8, 76.5, 72.7, 63.0, 47.7, 40.0, 29.4, 27.7, 17.2.

3.5. Ring Opening Polymerization of Lactide and Carbonate Monomer

3.5.1. Purification of Lactide Monomer

Lactide monomer (5 g, 0.034 mol) and toluene (6 mL) was stirred under reflux at 110 ^oC. After dissolving of lactide in toluene, solution was stirred and allowed to come room temperature. Then, it was filtered with a sintered glass funnel. Solid part was redissolved in toluene (6 mL) again under reflux at 110 ^oC. This process was followed three times and white pure solid was obtained (3.5 g).

3.5.2. Polymerization Initiated by Benzyl Alcohol (14)

The azide-containing monomer **(13)** (0.05 g, 0.2 mmol) and lactide (0.57 g, 3.8 mmol) were dissolved in anhydrous CH_2Cl_2 (3 mL). TU (0.04 g, 0.1 mmol) was added to the reaction mixture as a catalyst. Benzyl alcohol (1.1 µl, 0.01 mmol) as an initiator. Then, DBU (15.3 µl, 0.1 mmol) was added to the mixture as a co-catalyst system. Reaction was stirred at room temperature for 20 h. Copolymerization reactions were done in glovebox under N_2. Resulting polymer was purified by precipitation in 9:1 ether/methanol solution. ^{1}H NMR and GPC were used for characterization. GPC (10K, PDI: 1.15). ^{1}H NMR (400 MHz, $CDCl_3$) δ 7.28 (s, 5H), 5.29 – 4.93 (m, 351.60H), 4.35 – 4.21 (m, 33.80H), 4.15 (d, *J* = 5.1 Hz, 16.97H), 3.33 (d, *J* = 6.7 Hz, 18.50H), 1.91 – 1.77 (m, 13.95H), 1.47 (ddd, *J* = 21.0, 11.8, 5.3 Hz, 1114.91H), 1.24 – 1.12 (m, 58.21H).

3.5.3. Polymerization Initiated by Benzyl Alcohol (15)

The azide-containing monomer **(13)** (0.15 g, 0.6 mmol) and lactide (0.8 g, 5.4 mmol) were dissolved in anhydrous CH_2Cl_2 (3 mL). 1-(3,5-bis(trifluoromethyl)phenyl)-3-cyclohexyl-2-thiourea (TU, catalyst) was synthesized according to the previously reported literature procedure [46]. TU (0.05 g, 0.15 mmol) was added to the reaction mixture as a catalyst. After that benzyl alcohol (1.5 µl, 0.015 mmol) as added as an initiator. Then, DBU (22 µl, 0.15 mmol) was added to the mixture as a co-catalyst system. Reaction was stirred at room temperature for 20 h. Copolymerization reactions were done in glovebox under N_2. Resulting polymer was purified by precipitation in 9:1 ether/methanol solution. ^{1}H NMR and GPC were used for characterization. GPC (11K, PDI: 1.33). ^{1}H NMR (400 MHz, $CDCl_3$) δ 7.39 – 7.26 (m, 5H), 5.31 – 4.96 (m, 349.87H), 4.33 (d, *J* = 25.0 Hz, 56.9H), 4.20 (d, *J* = 4.9 Hz, 29.26H), 3.36 (s, 28.11H), 1.92 – 1.85 (m, 28.44H), 1.53 (dd, *J* = 21.8, 12.4 Hz, 1067.95H), 1.23 (s, 65.8H).

3.5.4. Polymerization Initiated by Benzyl Alcohol (16)

The azide-containing monomer **(13)** (0.2 g, 0.8 mmol) and lactide (0.48 g, 3.2 mmol) were dissolved in anhydrous CH_2Cl_2 (4 mL). TU (0.04 g, 0.1 mmol) was added to the reaction mixture as a catalyst. After that benzyl alcohol (1 µl, 0.01 mmol) as an initiator. Then, DBU (15 µl, 0.1 mmol) was added to the mixture as a co-catalyst system. Reaction was stirred at room temperature for 20 h. Copolymerization reactions were done in glovebox under N_2. Resulting polymer was purified by precipitation in 9:1 ether/methanol solution. ^{1}H NMR and GPC were used for characterization. GPC (8.28K, PDI: 1.3). ^{1}H NMR (400 MHz, $CDCl_3$) δ 7.22 (s, 5H), 5.10 (s, 186.22H), 4.25 (s, 95.51H), 4.16 (s, 47.32H), 3.32 (s, 47.51H), 1.84 (s, 42.64H), 1.50 (s, 562.18H), 1.19 (s, 103.61H).

3.5.5. Polymerization Initiated by Poly (ethylene glycol) Methyl Ether (17)

The azide-containing monomer **(13)** (0.1 g, 0.4 mmol) and lactide (0.54 g, 3,6 mmol) were dissolved in anhydrous CH_2Cl_2 (4 mL). Poly (ethylene glycol) methyl ether was added (7.5 mg, 0.010 mmol) as an initiator. Then, DBU (15 µl, 0.10 mmol) was added to the mixture as a co-catalyst. Reaction was stirred at room temperature for 20 h. Copolymerization reactions were done in glovebox under N_2. Resulting polymer was purified by precipitation in 9:1 ether/methanol solution. ^{1}H NMR and GPC were used for characterization. GPC (12K, PDI: 1.3). ^{1}H NMR (400 MHz, $CDCl_3$) δ 5.29 – 4.95 (m, 1477.87H), 4.31 (t, J = 17.1 Hz, 345.48H), 4.20 (d, J = 4.9 Hz, 168.51H), 3.62 (d, J = 5.4 Hz, 62H), 3.37 (d, J = 6.4 Hz, 176.04H), 1.97 – 1.82 (m, 156.39H), 1.64 – 1.42 (m, 4693.49H), 1.24 (s, 246.51H).

4. RESULTS AND DISCUSSIONS

4.1. Synthesis of Azide Containing Carbonate Monomer

General scheme of synthesis of azide containing carbonate monomer is shown in Figure 4.1. The monomer was synthesized according to the previously reported literature procedures as were cited them in experimental section.

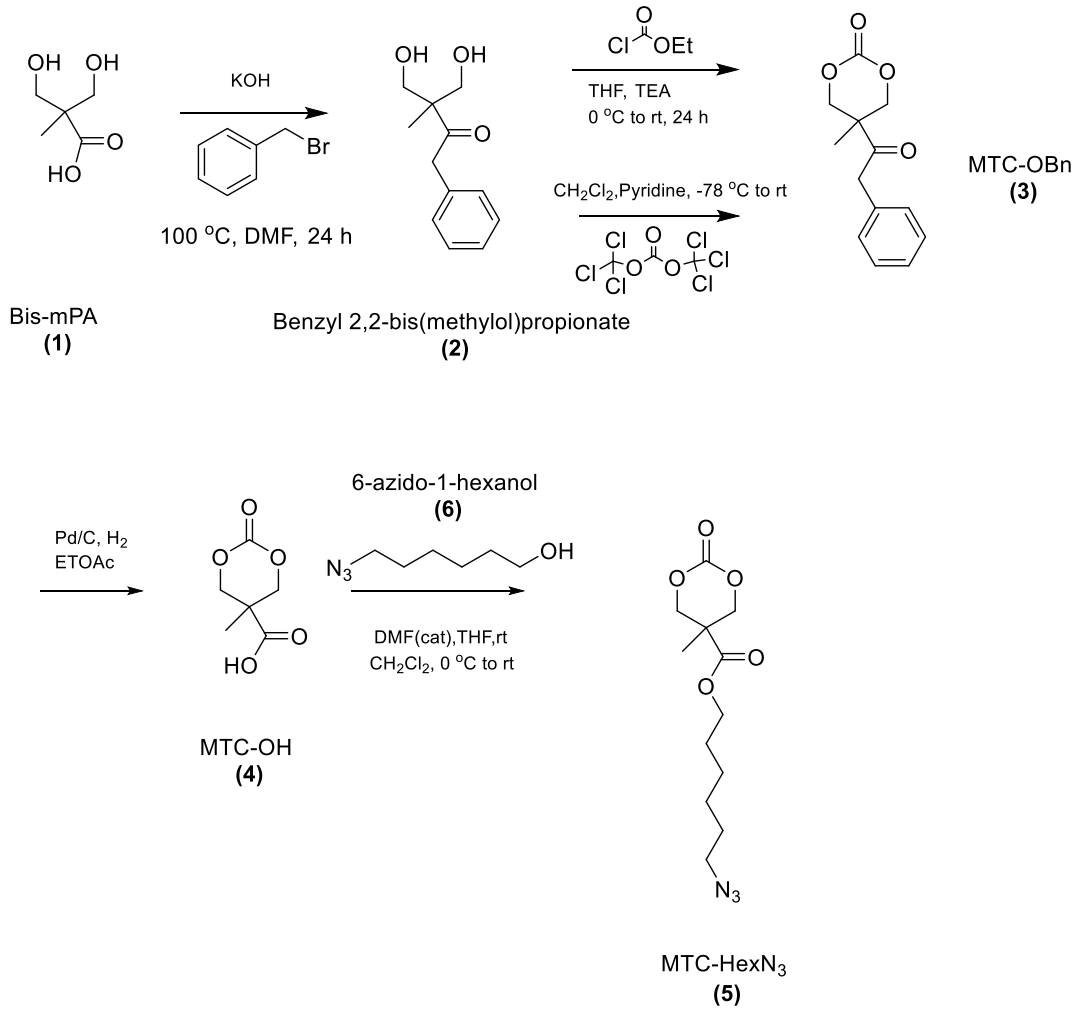

Figure 4.1. General scheme of synthesizing azide containing carbonate monomer.

Benzyl 2,2-bis(methylol)propionate **(2)** was synthesized according to the reported literature procedure [43]. In an overall, yield was 76%. Some of the product didn't precipitate in toluene since it was recrystallized from toluene. In this case, column chromatography was done after recrystallization to prevent loss of product. After synthesizing **(2)**, MTC-OBn **(3)** was synthesized with two methods (Method A and B) [43]. Initially, Method A was used however the product couldn't be purified via neither column chromatography nor recrystallization. According to the previous literature example, ethylacetate was used for recrystallization. However, recrystallization from ethylacetate couldn't totally purify the product. Two or three spots were obtained after the recrystallization. Column chromatography was used, however MTC-OBn could be obtained with a very low yield (45%) since the compounds were very close in polarity and they could not be separated. Therefore, Method B was used because it didn't give too many by-products as many as first method. Recrystallization from ethylacetate again couldn't purify MTC-OBn (two or more spots in TLC after recrystallization) and yield was 69%. Since triphosgene is very toxic and it can cause skin burns, eye damage and it is fatal if inhaled, Method A was revisited for the reaction and solvent was changed for recrystallization from ethylacetate to diethylether that could completely purify product with 80% yield. Also, the yield of first method was higher than the yield of second method. ^{1}H NMR was used for determining that product was obtained in pure form (Figure 4.2).

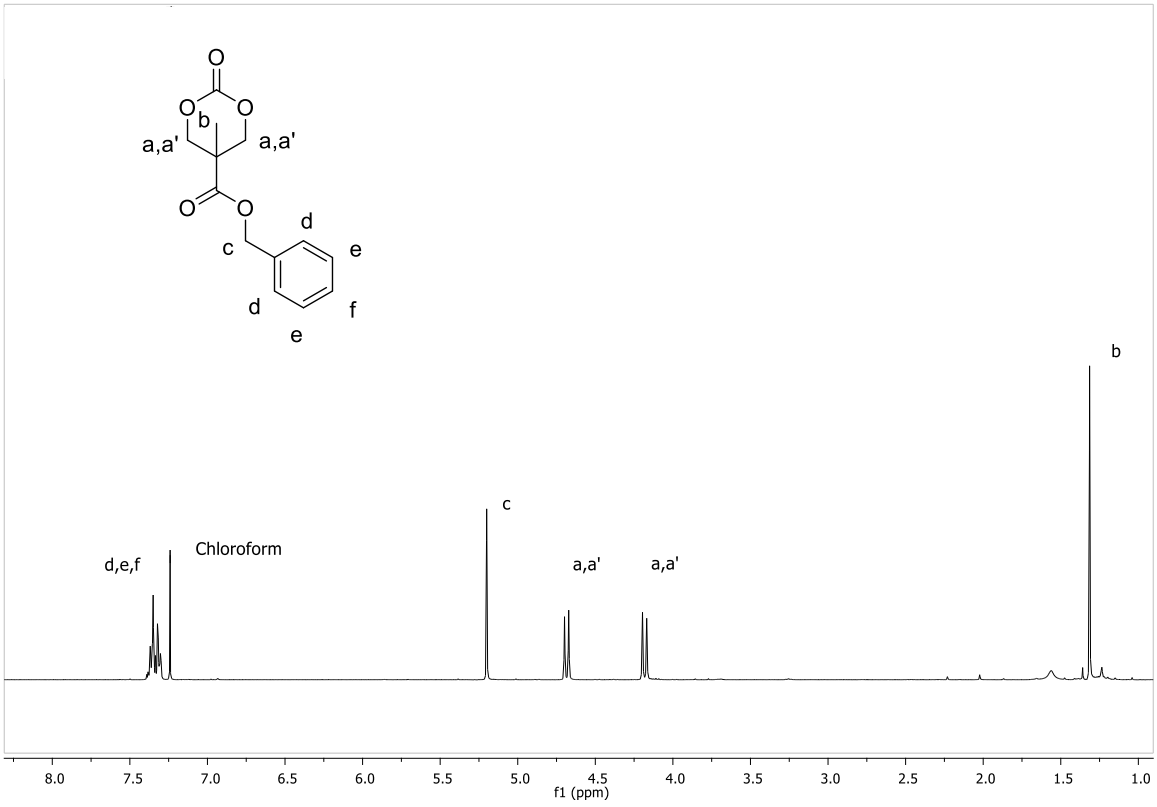

Figure 4.2. ^{1}H NMR spectrum of MTC-OBn **(3).**

After synthesizing MTC-OBn **(3)**, MTC-OH **(4)** was synthesized according to the previously reported literature procedure [44]. Reactant of this reaction, MTC-OBn, must be totally pure for obtaining pure MTC-OH because MTC-OH did not dissolve in CH_2Cl_2 or in EtOAc for loading onto column for purification using chromatography. Therefore, column chromatography could not be used to purify MTC-OH. When the reaction was undertaken with absolutely pure MTC-OBn, MTC-OH was obtained in pure form in 65% yield and there was no need for further purification. ^{1}H NMR was used for deducing that product was obtained with high purity (Figure 4.3).

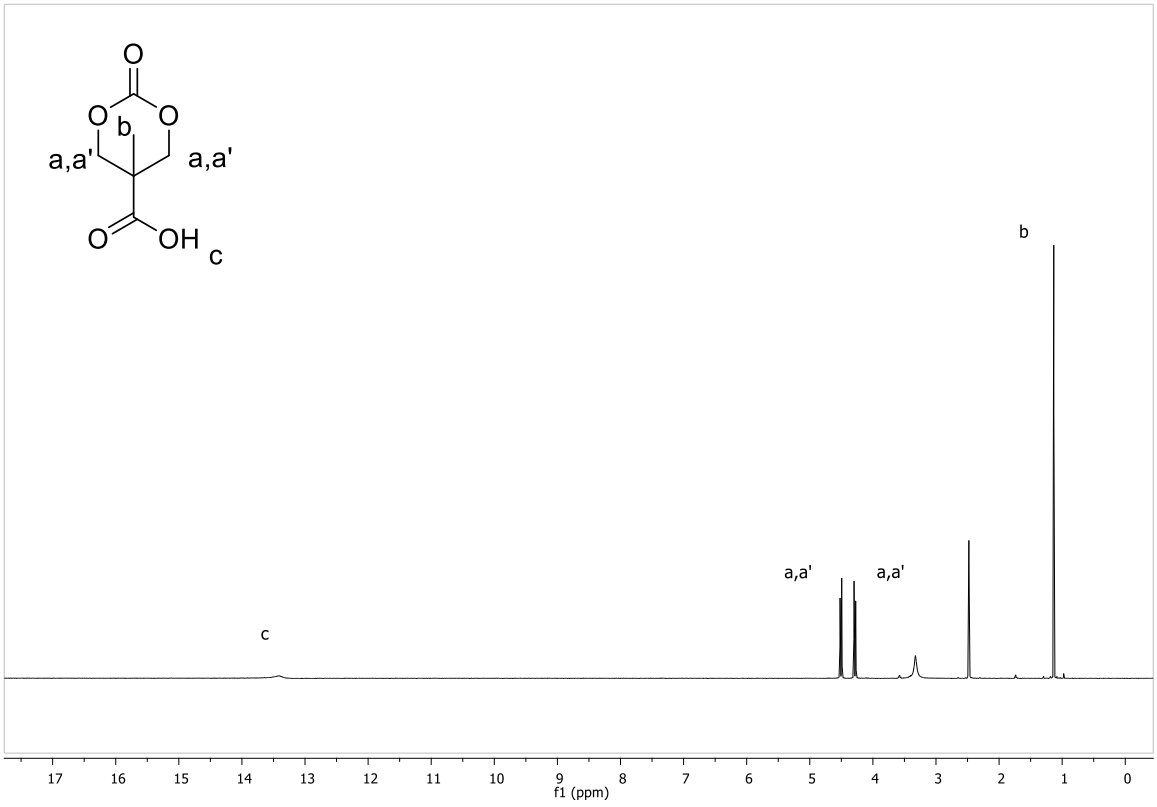

Figure 4.3. ^{1}H NMR spectrum of MTC-OH **(4)**.

After obtaining MTC-OH **(4)**, 6-azido-1-hexanol **(6)** was synthesized with 93% yield (Figure 4.4). 6-azido-1-hexanol was generally obtained in pure form after the reaction.

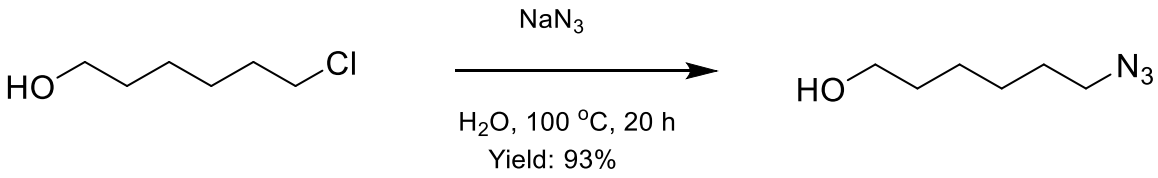

Figure 4.4. Synthesis of 6-azido-1-hexanol **(6)**.

After synthesizing 6-azido-1-hexanol **(6)**, azide containing carbonate monomer **(5)** was synthesized using a previously reported esterification procedure of MTC-OH [45]. The yield of this reaction could not be calculated because final product could not be purified with

either crystallization or column chromatography. At the end, there were at least 3 compounds in the media and there was always the unreacted initial reagent (MTC-OH). The compound could not be purified by column chromatography since the compound decomposed during the chromatography process. Therefore, a second method was followed for the synthesis.

4.2. Second Method of Synthesis of Azide-Containing Carbonate Monomer

General scheme of second route for synthesizing azide containing carbonate monomer is shown in Figure 4.5. The monomer was synthesized according to the previously reported literature procedures cited in the experimental section.

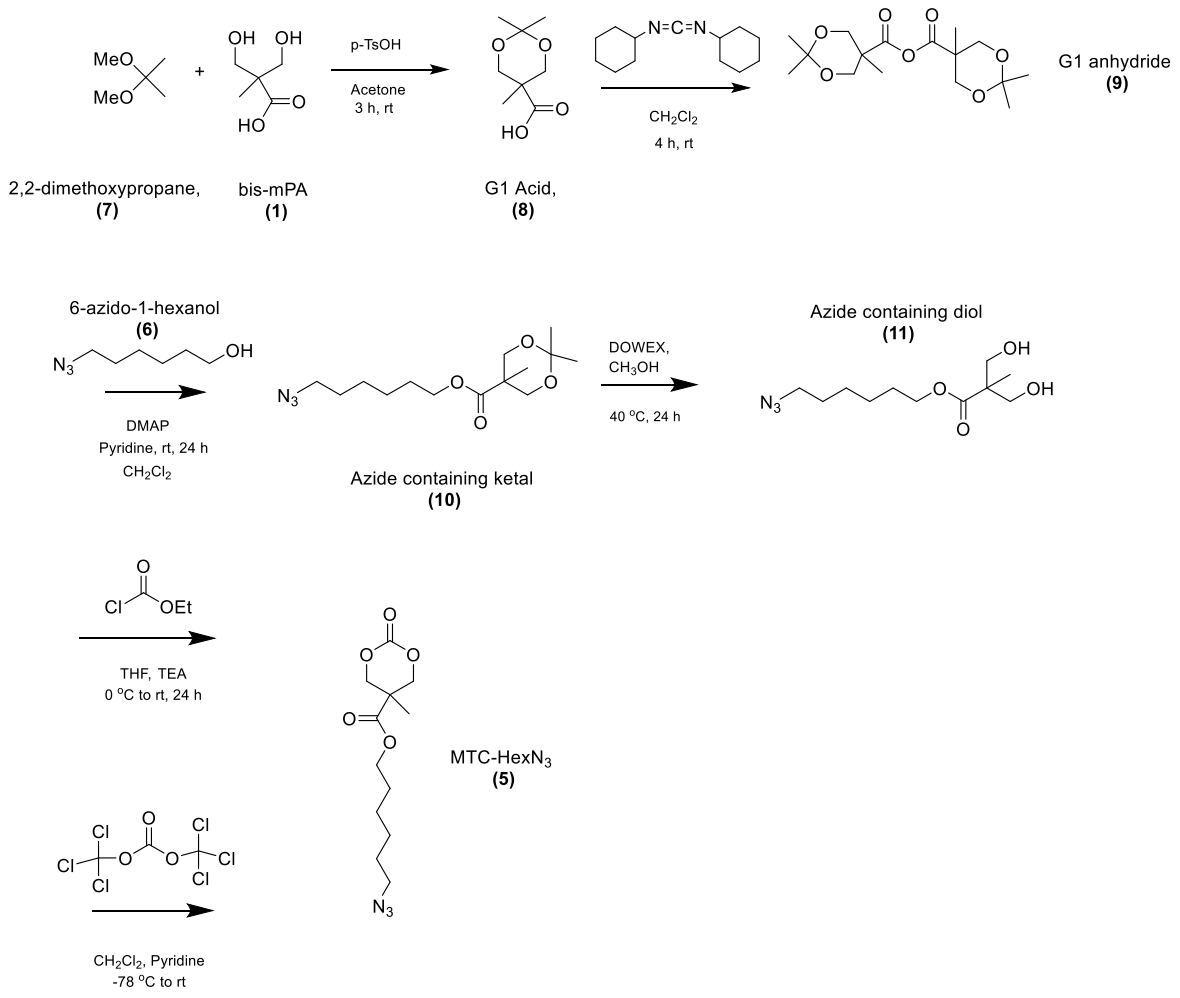

Figure 4.5. Second route for synthesizing azide containing carbonate monomer (5)

First, G1 acid **(8)** was synthesized according to the previously reported literature procedure with 58% yield [47]. After that G1 anhydride **(9)** was synthesized with a yield of about 85%. Obtained anhydride was reacted with azido hexanol **(6)** in the presence of DMAP in anhydrous CH_2Cl_2 and pyridine. At least three spots were obtained and the spots were very close to each hence it was hard to purify this compound. Equivalences of the reactants were varied in order to obtain more pure products. After that, column chromatography was done to obtain pure product in 74% yield. In the next step, DOWEX-H^+ was used to deprotect the ketal **(10)** and obtain diol **(11)** with 77% yield after purification using column chromatography. After this, the final step for obtaining the monomer was investigated. In this step, there were two ways to follow as mentioned before. No pure product could be obtained using any of the methods.

However, at least one by-product was obtained with the second method of synthesizing carbonate monomer. It was assumed that the long hydrocarbon chain was responsible for the poor efficiency of crystallization; therefore, synthesis of an azide containing carbonate monomer with a shorter chain was investigated.

4.3. Synthesis of Another Carbonate Monomer Containing Azide

Another azide containing carbonate monomer was synthesized with the hope of purification by recrystallization. Firstly, 3-azido-1-hexanol **(12)** was synthesized. The procedure was similar to the procedure of synthesizing 6-azido-1-hexanol **(6)**. Generally, pure product could be obtained after the reaction (Figure 4.6). Sometimes, column chromatography was made for purification. ^{1}H NMR was used for characterization (Figure 4.7). Yield was 89%.

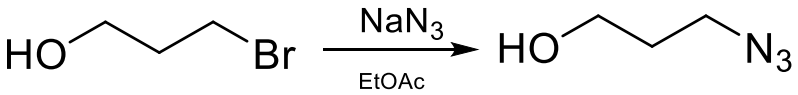

Figure 4.5. Synthesis of 3-azido-1-propanol **(12)**.

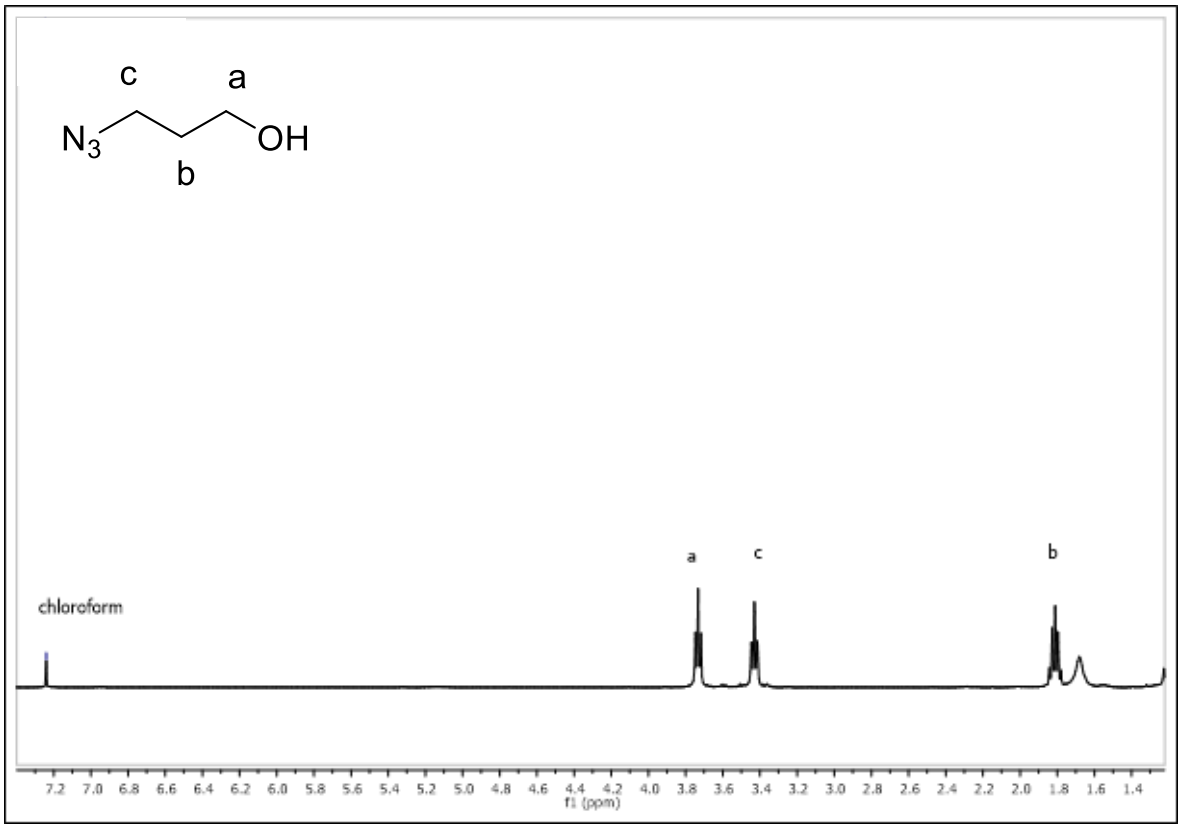

Figure 4.6. ^{1}H NMR spectrum of 3-azido-1-propanol **(12)**.

The monomer was synthesized by coupling carbonate-containing acid **(4)** with 3-azido-1-propanol **(12)** (Figure 4.8). In spite of the short alkyl chain, the compound could not be recrystallized. Hence, column chromatography was used to obtain pure monomer **(13)** in 55% yield. The yield could not be increased due to the decomposition during chromatography.^{1}H NMR (Figure 4.9), ^{13}C-NMR (Figure 4.10) and FTIR (Figure A.1) were used for characterization.

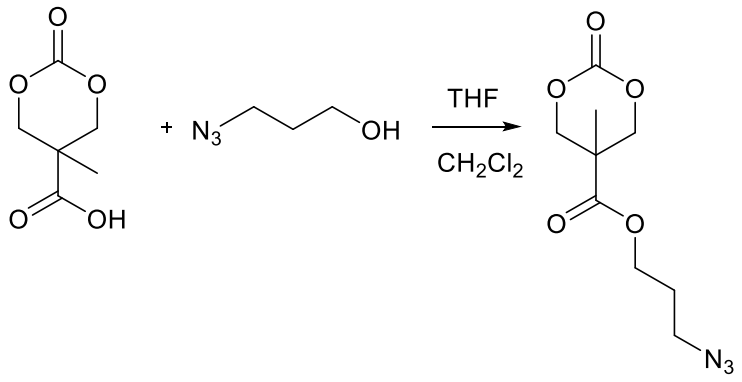

(4) **(12)** MTC-PropN_3, **(13)**

Figure 4.7. Synthesis of another carbonate monomer containing azide **(13)**.

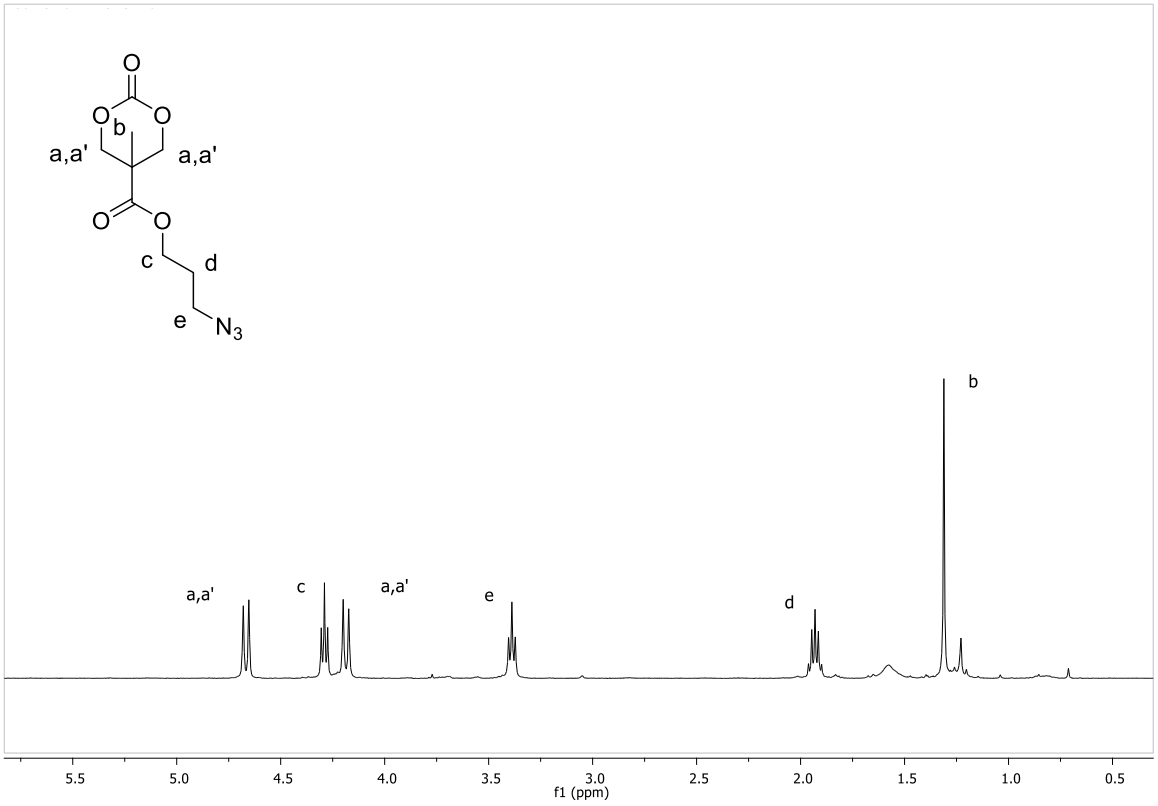

Figure 4.8. ^{1}H NMR spectrum of carbonate monomer **(13)**.

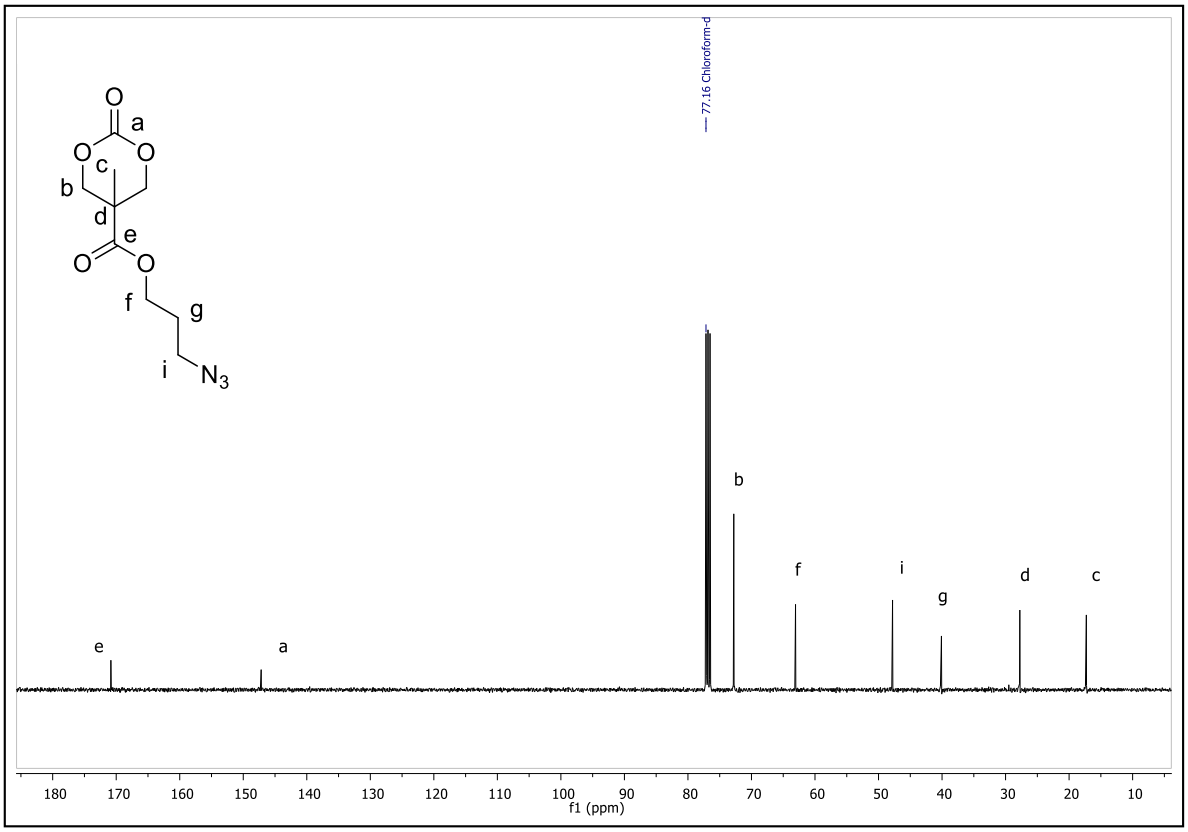

Figure 4.9. ^{13}C NMR spectrum of carbonate monomer **(13)**.

After obtaining the pure azide containing monomer **(13**), it was copolymerized with the lactide monomer (Figure 4.11). The ratio of lactide and carbonate monomer was maintained as 95:5 **(14)**, 90:10 **(15)** and 80:20 **(16)** (Table 4.1). The copolymer was obtained in pure form after precipitation in 9:1 diethylether:methanol solution. ^{1}H NMR (Figure 4.12, 4.13, 4.14), GPC (Figure A.2, A.3, A.4) and FTIR (Figure 4.18) were used for characterization. GPC results were 10K, PDI: 1.15 for copolymer **14**; 11K, PDI: 1.24 for copolymer **15** and 8.28K, PDI: 1.3 for copolymer **16.**

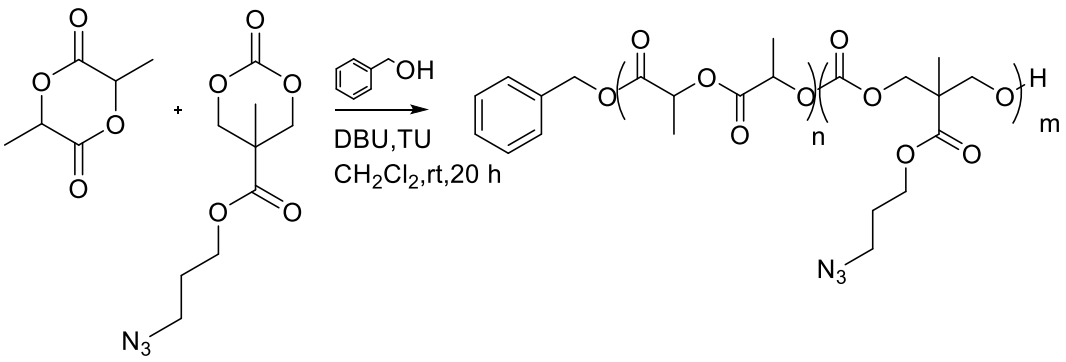

Figure 4.10. Synthesis of copolymer initiated by benzyl alcohol **(14), (15),(16)**.

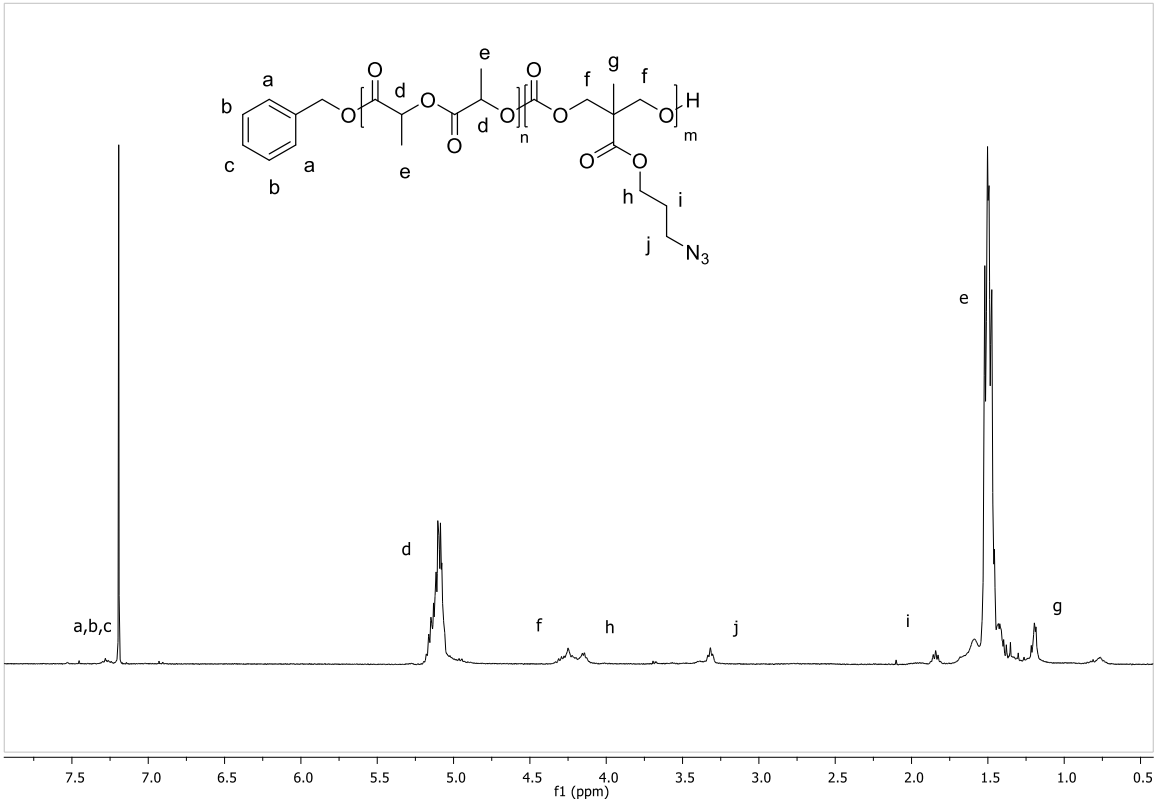

Figure 4.11. ^{1}H NMR spectrum of 5% azide containing copolymer **(14)**.

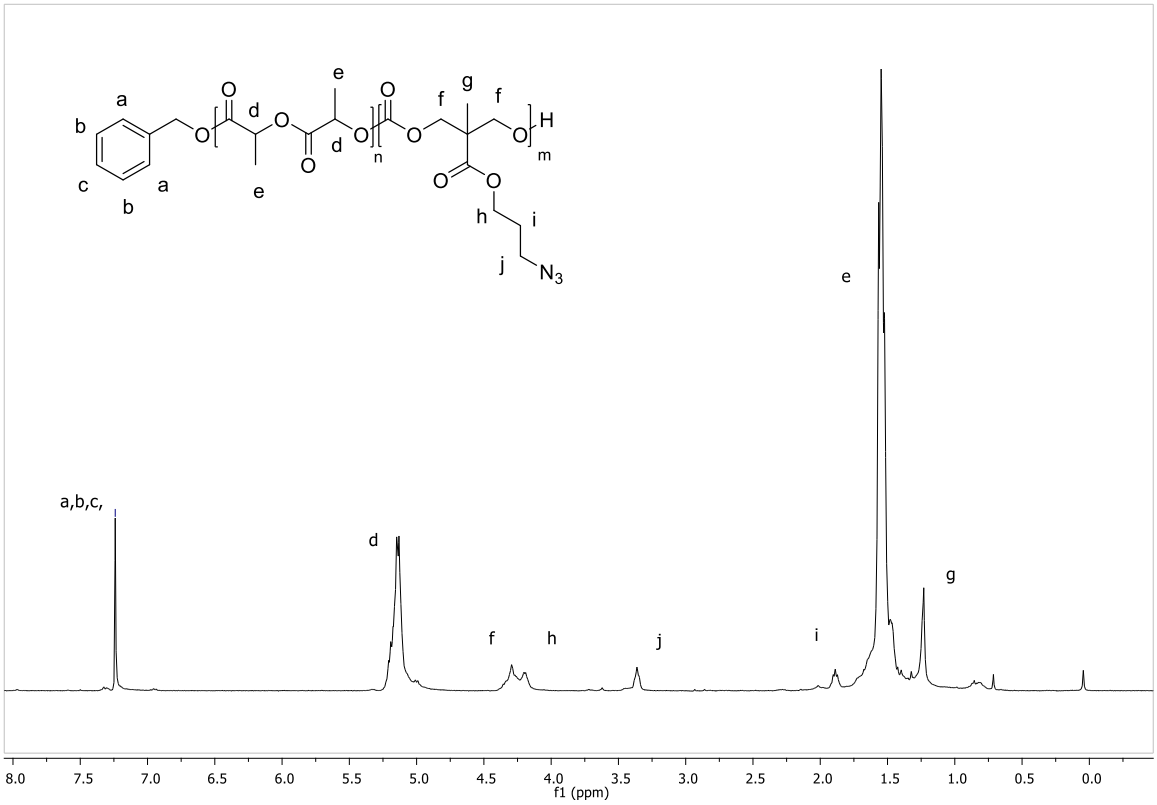

Figure 4.12. ^{1}H NMR spectrum of 10% azide containing copolymer **(15)**.

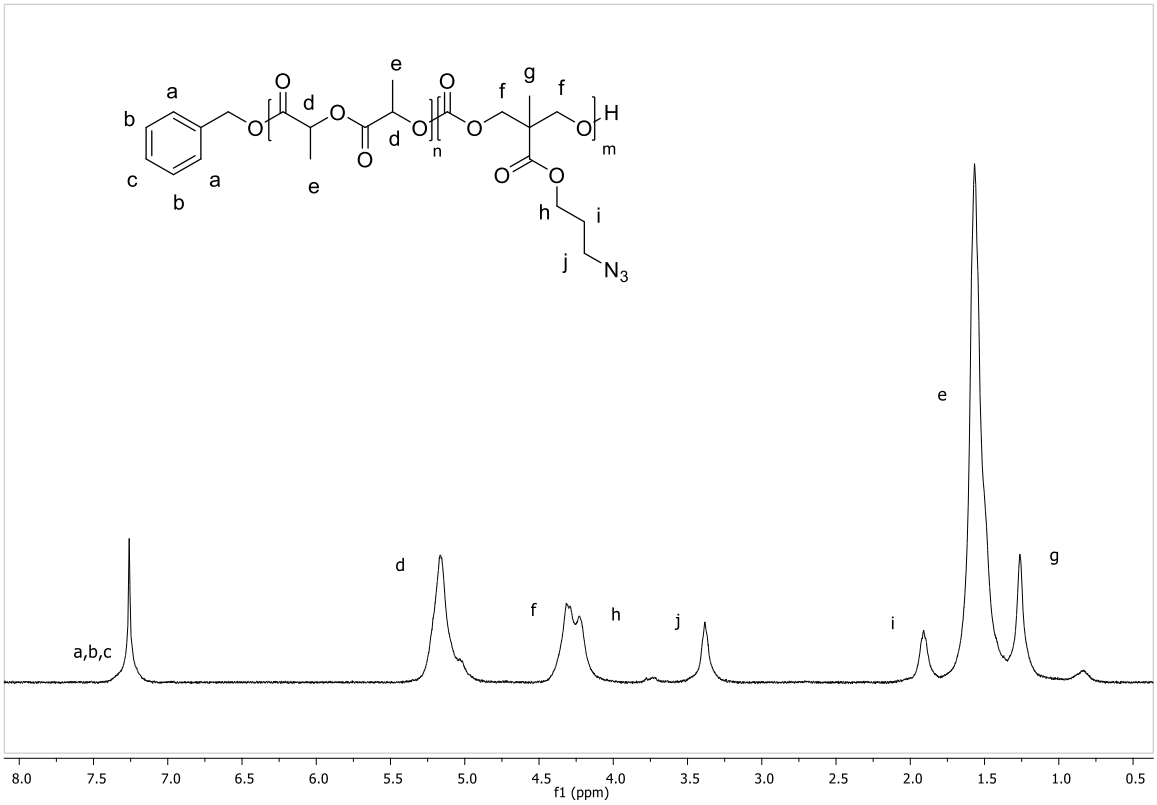

Figure 4.13. ^{1}H NMR spectrum of 20% azide containing copolymer **(16)**.

Table 4.1. Characteristic Data for Polymerizations Reactions.

	Lactide	**Azide-containing carbonate monomer**	**DBU**	**TU**	**Benzyl Alcohol (Initiator)**	**Poly(ethylene glycol) methyl ether (Initiator)**	**M_n(GPC) KDa**	**M_w/ M_n**
P1	190	10	5	5	0.5	-	10.0	1.15
P2	190	10	5	5	0.5	-	8.0	1.38
P3	190	10	5	5	0.5	-	9.4	1.33
P4	180	20	5	5	0.5	-	11.3	1.24
P5	180	20	5	5	0.5	-	11.6	1.33
P6	180	20	5	5	0.5	-	10.4	1.32
P7	180	20	5	-	-	0.5	12.1	1.35
P8	160	40	5	5	0.5	-	8.3	1.37

Additionally, poly (ethylene glycol) methyl ether was also used to initiate polymerization. The ratio of lactide and carbonate monomer was 90:10. Purification was done via precipitation in 9:1 diethylether:methanol solution. Poly (ethylene glycol) methyl ether was used as an initiator in order to impart antibiofouling property to the nanofibers (Figure 4.15). Because, copolymer of azide containing carbonate monomer and lactide was hydrophobic. One can expect proteins to bind non-specifically to these fibers. Therefore, proteins, which contain hydrophobic patches, will attach to nanofiber that doesn't have any ligand on it because of the hydrophobic-hydrophobic interaction. To prevent this nonspecific adsorption, polymers were synthesized with PEG containing methyl ether as an initiator. PEG content increased hydrophilicity of the nanofiber and prevented nonspecific adsorption of biomolecules. ^{1}H NMR (Figure 4.16), GPC (Figure A.5) and FTIR (Figure A.6) were used for characterization. Molecular weight of copolymer was found to be 12K and PDI was 1.3.

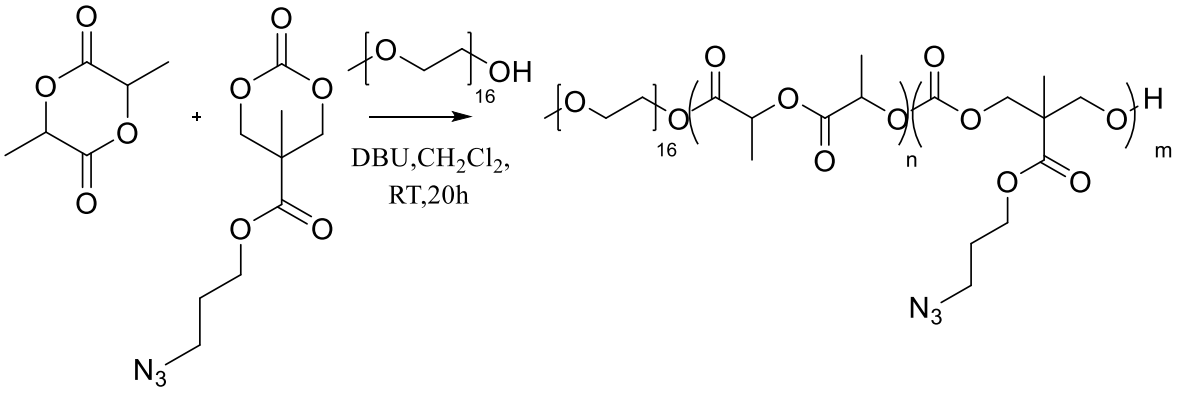

(17)

Figure 4.14. Synthesis of copolymer **(17)**.

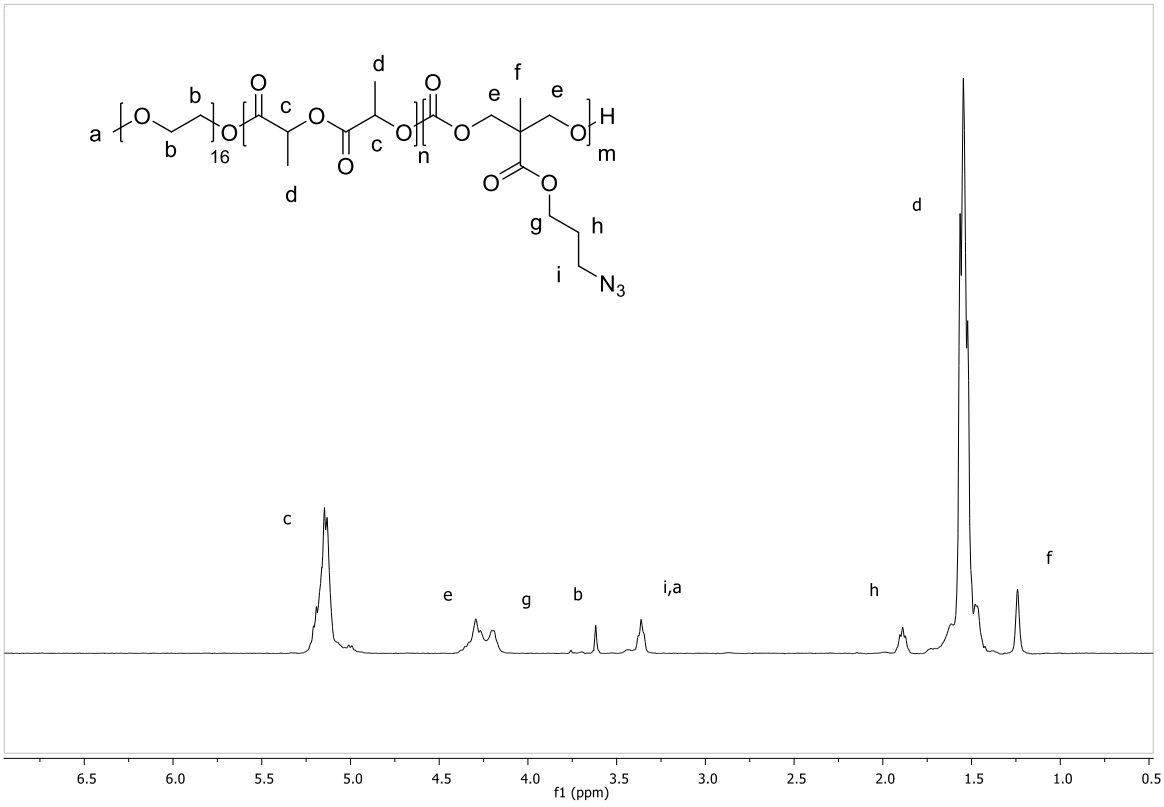

Figure 4.15. ^{1}H NMR spectrum of copolymer **(17)**.

4.4. Preparation and Functionalization of Nanofibers

Azide containing polymers were spun via electrospinning with a concentration of 58 wt % polymer in chloroform. Applied voltage was 15 kV, distance between tip of syringe and collector was 15 cm, flow rate was 0.01mL/min. First obtained fibers had an average diameter of 1.7± 0.3 μm, they weren't in nanoscale (Figure 4.17). However, firstly, survival of azide groups during electrospinning was investigated. FTIR spectra of polymer solution before electrospinning (Figure 4.18) and fiber after electrospinning (Figure 4.19) were taken. These spectras proved that azide groups survived during electrospinning.

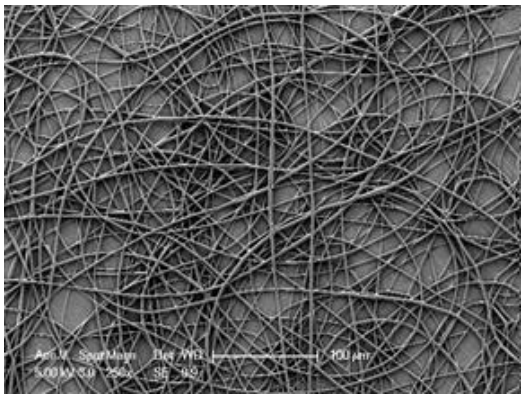

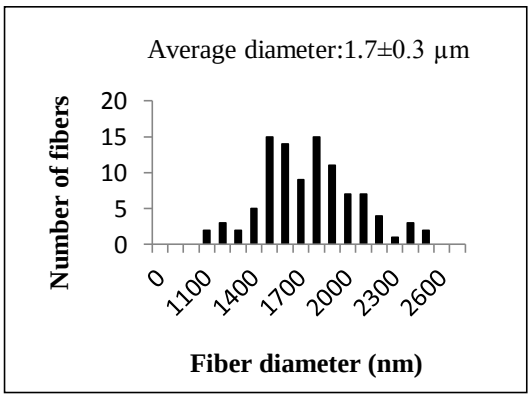

Figure 4.16. SEM images of fibers, 58 wt % polymer in chloroform.

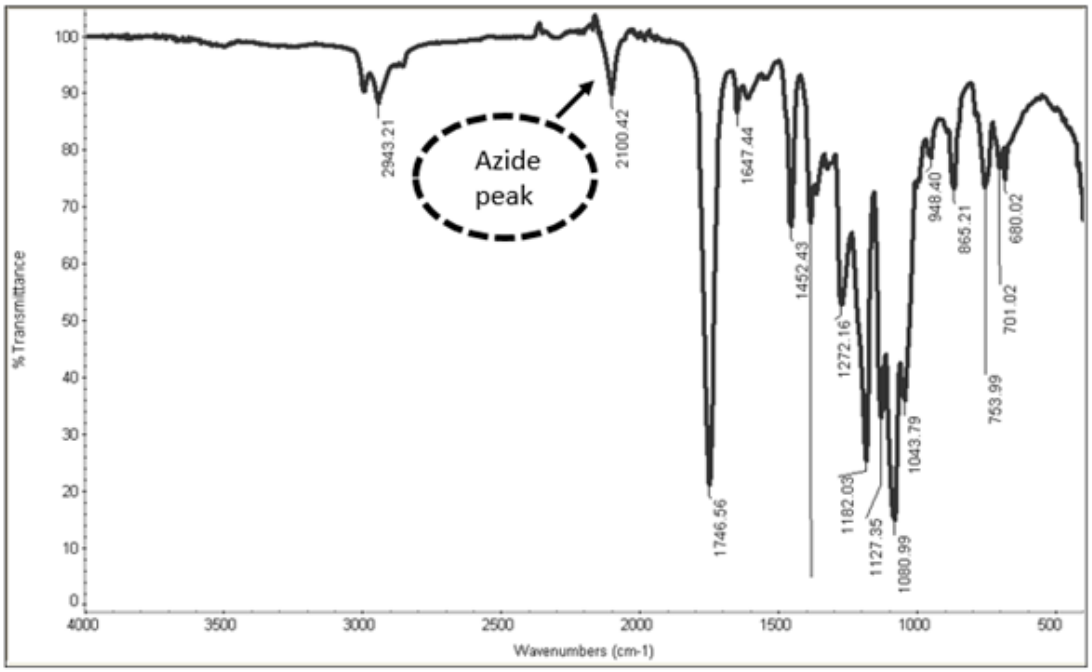

Figure 4.17. FTIR spectrum of azide containing copolymer **(15)**.

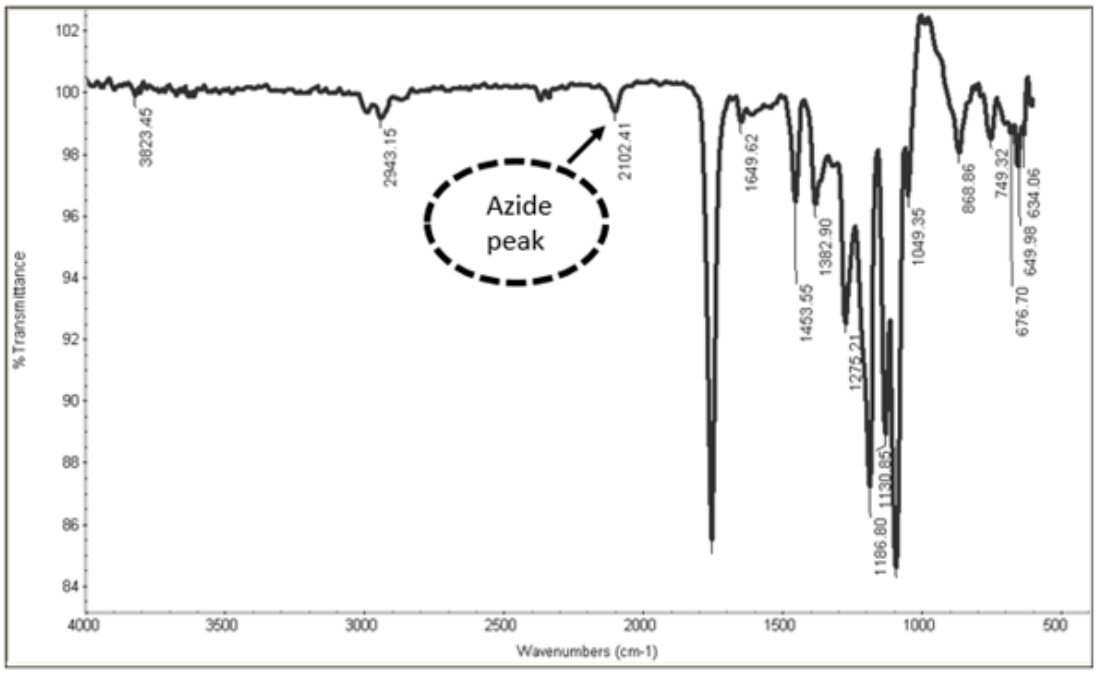

Figure 4.18. FTIR spectrum of azide containing nanofibers **(15)**.

After ensuring the survival of azide groups during electrospinning, diameters of fibers were decreased with the help of decreasing polymer concentration of the solution (50 wt % polymer in chloroform). Second spun nanofibers had an average diameter of 1.174 µm±294 nm. SEM images of nanofibers were taken (Figure 4.20A).

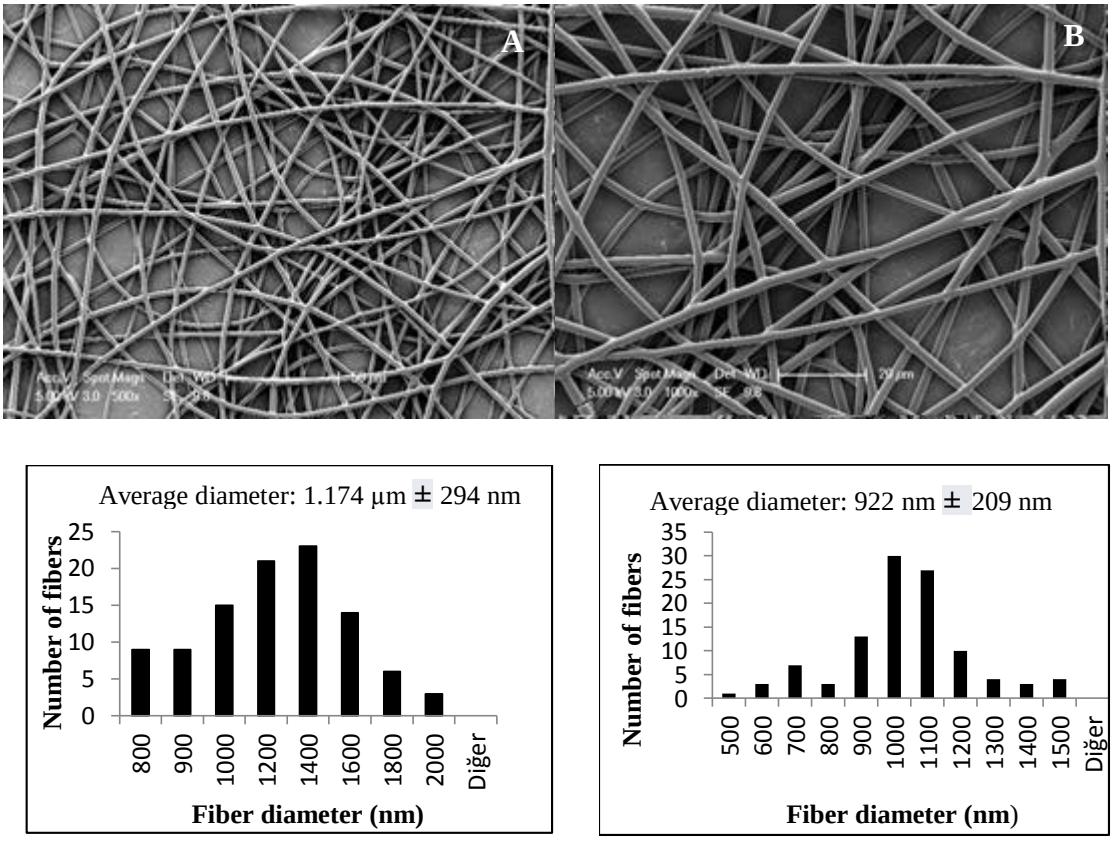

Figure 4.19. SEM images of nanofibers; A: 50 wt % polymer in chloroform, B: 43 wt % polymer in chloroform.

Polymer solution was diluted more (43 wt % polymer in chloroform) in order to decrease diameter of fibers more. SEM images were taken again (Figure 4.20B). Average diameter was found as 922 nm± 209 nm. Polymer solution was diluted again (40 wt % polymer in chloroform) in order to decrease the diameter of nanofibers. SEM images of nanofibers were taken (Figure 4.21) Average diameter was found to be 702 nm±165 nm when concentration was 40 wt % polymer in chloroform. SEM images confirmed highly

uniform structure of the final nanofibers. SEM images of nanofibers that was spun from copolymer **(14)**, **(15)** and **(16)** showed highly uniform structures (Figure 4.22).

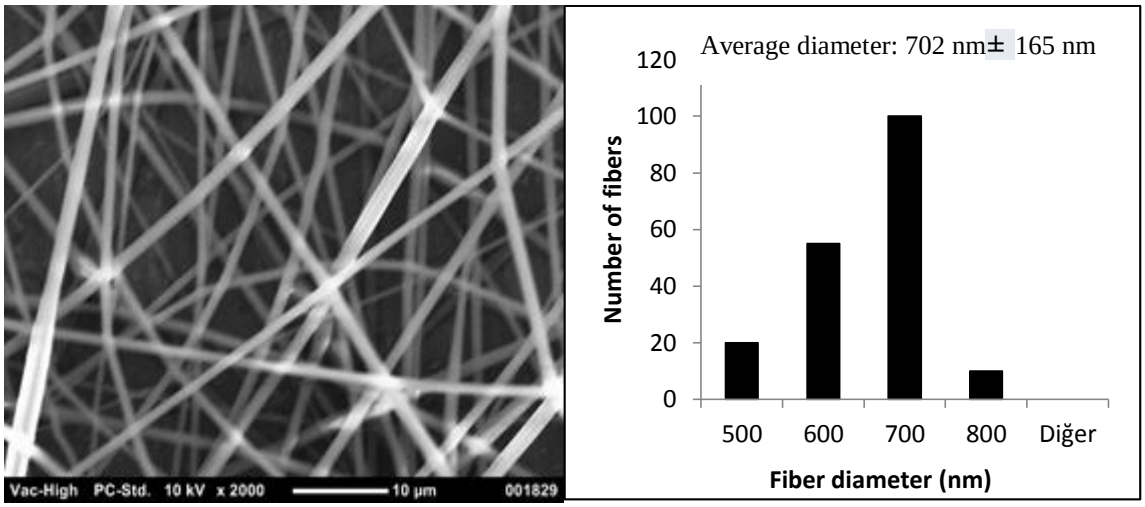

Figure 4.20. SEM images of nanofibers, 40 wt % polymer in chloroform.

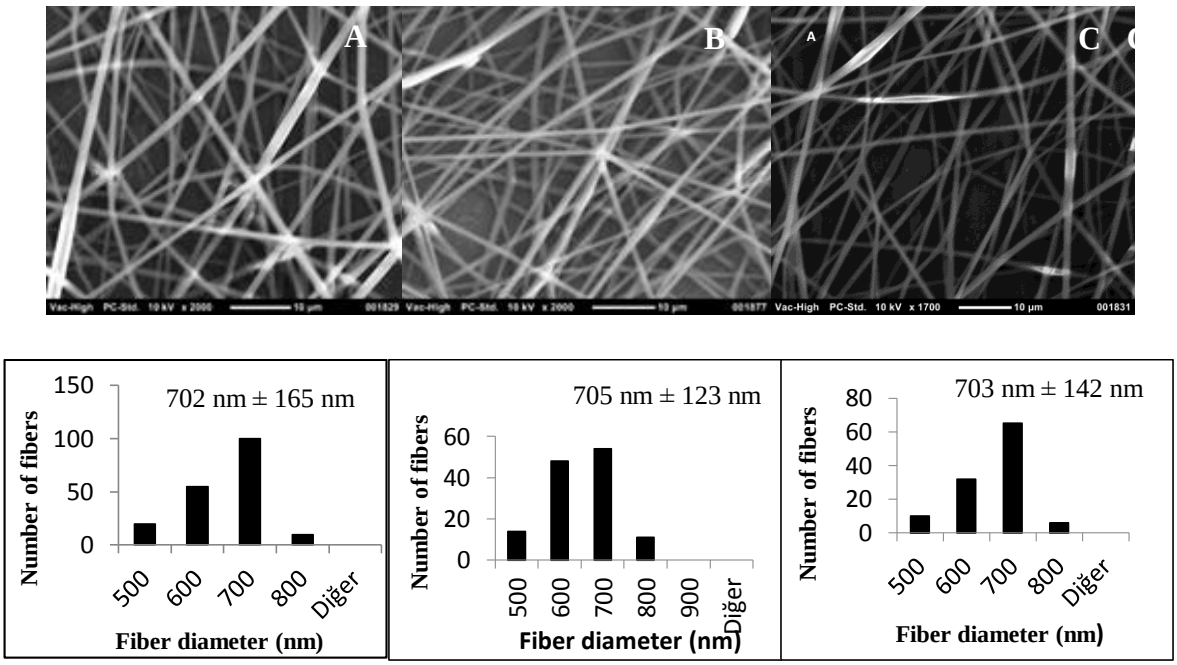

Figure 4.21. SEM images of nanofibers 5% (A), 10% (B), 20% (C) azide containing nanofibers.

4.4.1. Functionalization of Nanofibers

For the functionalization of nanofibers, azide containing fibers were first treated with a DIBO-containing fluorescent dye, DBCO-PEG4-Carboxyrhodamine 110 (Figure 4.24). 15 µl DBCO-PEG4-Carboxyrhodamine 110 was dropped on the azide containing nanofibers. After 4.5 h in the dark, fibers were washed with water in order to remove excess dye and examined under fluorescence microscope. To check if the specific adsorption of the fluorescent dye on the nanofibers was a result of the azide-alkyne cycloaddition, a control experiment was done with the same conditions on the nanofibers that were spun from polylactide only. Fibers were examined under fluorescent microscope (Figure 4.23). Results showed that there was negligible nonspecific adsorption of fluorescent dye on the non-reactive nanofibers.

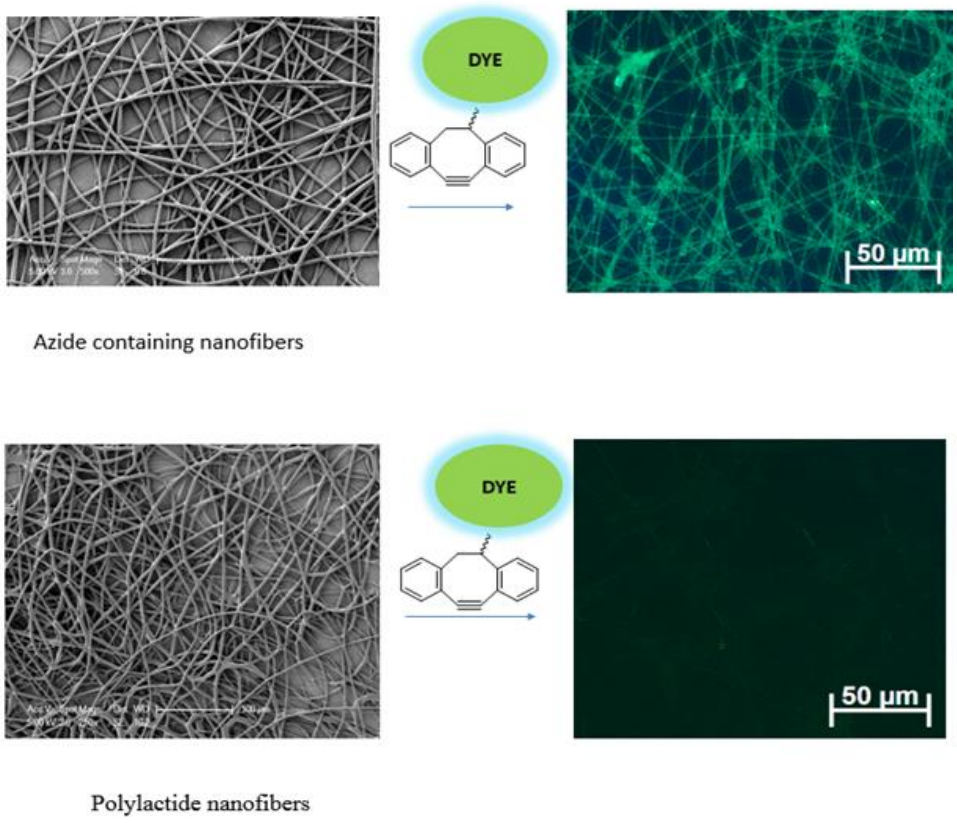

Figure 4.22. Functionalization of nanofibers.

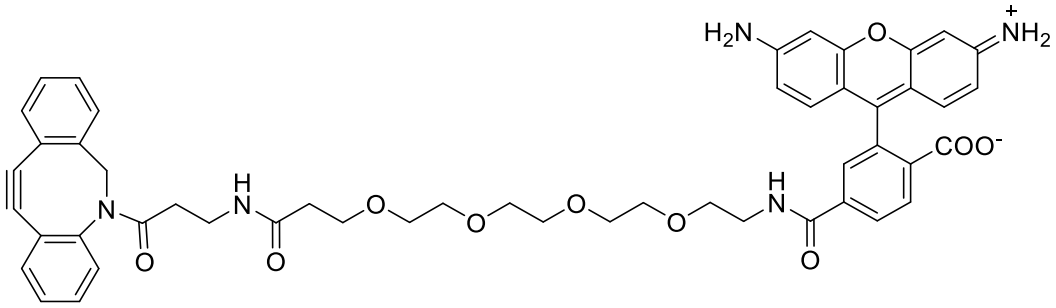

Figure 4.23. Chemical structure of DBCO-PEG4-Carboxyrhodamine 110.

4.4.2. Tunability of Nanofibers

To check the tunability of nanofiber functionalization by variation of amount of azide group on copolymer; 5% **(14)**, 10% **(15)** and 20% **(16)** azide containing polymers were electrospun, treated with 15 µl DBCO-PEG4-Carboxyrhodamine 110 solution for 4.5 h and evaluated under fluorescence microscope after washing with water (Figure 4.25). It was observed that, as azide group increased on nanofibers, intensity of the color increased because of more conjugation between alkyne part of DBCO-PEG4-Carboxyrhodamine 110 solution and azide groups on the nanofibers as a result of strain promoted azide-alkyne cycloaddition. Water contact angle measurements (Figure 4.26) were undertaken for characterization of hydrophobicity-hydrophilicity. Water contact angles were $104.3^0 \pm 3.2^0$ for 5% azide containing nanofibers, $99.92^0 \pm 5.8^0$ for 10% azide containing nanofibers and $85.7^0 \pm 4.1^0$ for 20% azide containing nanofibers, showing that increased polarity increased hydrophilicity (Figure 4.26).

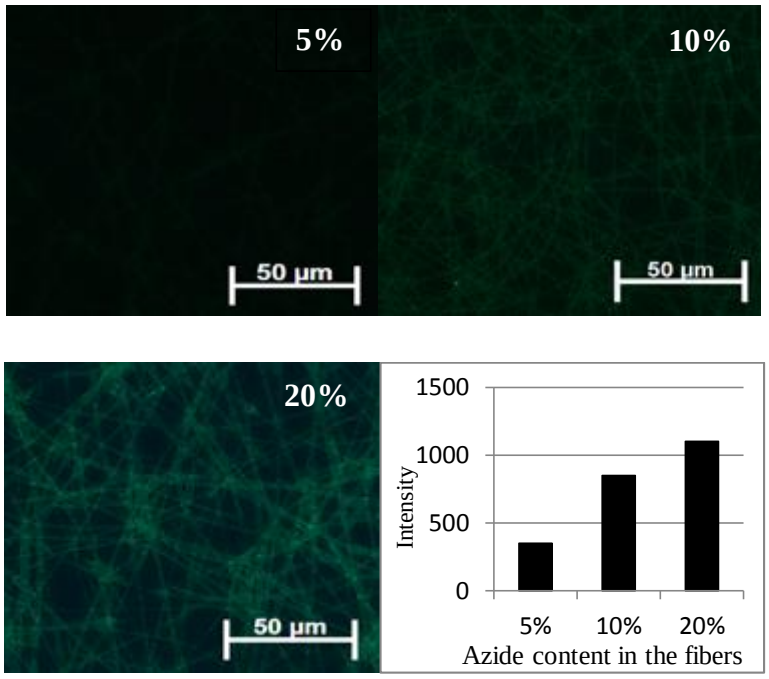

Figure 4.24. Fluorescence images of nanofibers and fluorescence intensity graph

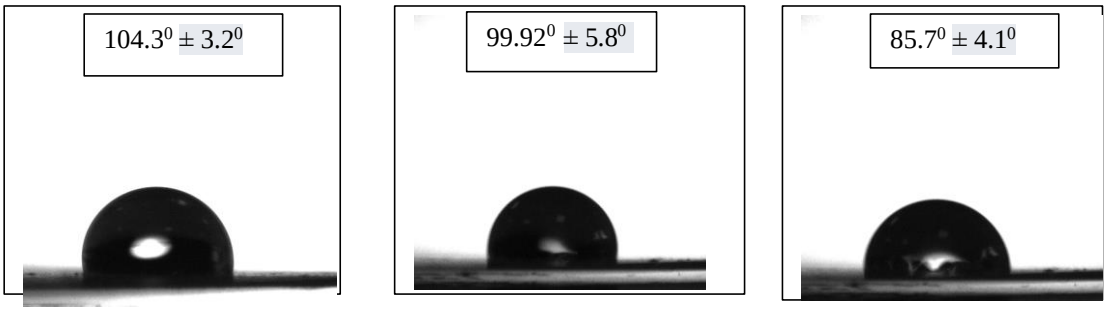

Figure 4.25. Water contact angle test of nanofibers; 5%, 10% and 20% azide containing nanofibers from left to right, respectively.

4.4.3. Biofunctionalization of Nanofibers

For biofunctionalization (Figure 4.28) of azide-containing nanofibers, TRITC-extravidin was used as a biomolecule (protein) and biotin (Figure 4.27A) was used because of the high affinity of extravidin for biotin. Nanofibers were electrospun from PEG-containing copolymer **(17)** in order to give anti-biofouling property to the nanofibers because the copolymer of azide-containing carbonate monomer and lactide was hydrophobic. One can expect proteins to bind non-specifically. Therefore, extravidin, which has hydrophobic domains will attach to nanofiber that does not have biotin on it because of the hydrophobic-hydrophobic interaction. To prevent this nonspecific adsorption, polymers were synthesized with PEG containing methyl ether as an initiator. PEG content increased hydrophilicity of the nanofiber and prevented nonspecific adsorption of extravidin. Immobilization of extravidin was confirmed from red color under fluorescence microscope. Alkyne (DIBO)-biotin (Figure 4.27B) was attached to the fibers via strain promoted azide-alkyne cycloaddition and immobilization of extravidin was due to the high affinity of extravidin for biotin.

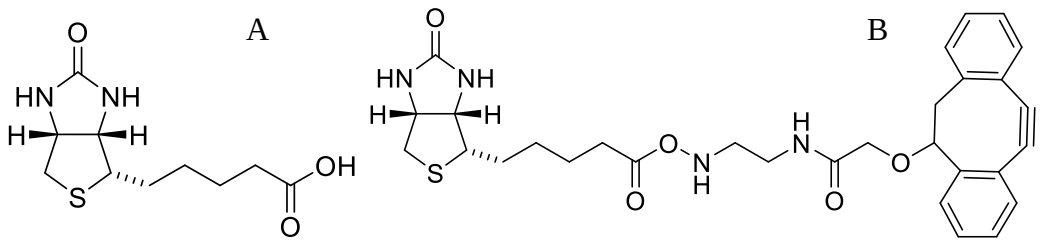

Figure 4.26. Chemical structure of biotin (A) and DIBO-Biotin (B).

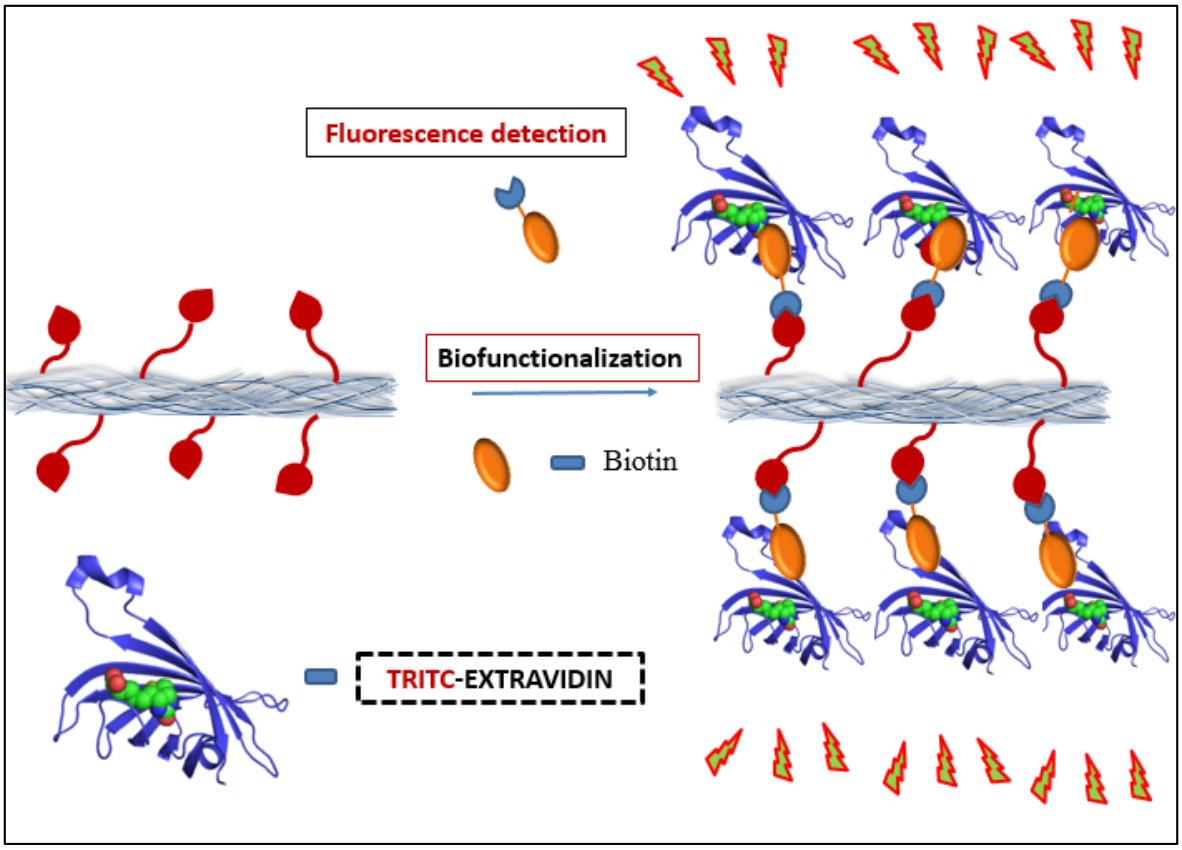

Figure 4.27. Schematic representation of biotin-directed biofunctionalization.

As a control experiment, both hydrophobic (electrospun from **15**) and more hydrophilic (electrospun from **17**) nanofibers were treated with 15 µl TRITC-extravidin (1mg/100mL) solution for 0.5 h in the dark, washed with water to remove unbound TRITC-Extravidin and examined under fluorescence microscope (Figure 4.29). It was observed that extravidin attached to the hydrophobic nanofibers nonspecifically (Figure 4.29A) because of the hydrophobic-hydrophobic interaction whereas it didn't attach to the PEG containing nanofibers because of the increased hydrophilicity and anti-biofouling property (Figure 4.29B).

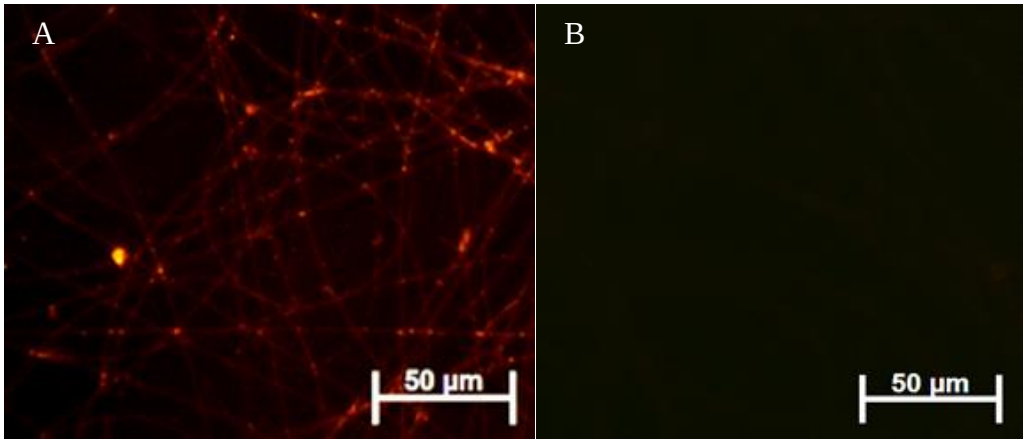

Figure 4.28. Fluorescence images of nanofibers; A: hydrophobic nanofibers, B: more hydrophilic nanofibers.

Hydrophobic nanofibers (electrospun from **15**) and more hydrophilic nanofibers (electrospun from **17**) were tested with water contact angle test that proved the difference between hydrophilicity of the nanofibers (Figure 4.30). The average contact angle of hydrophobic nanofibers was 99.92 ± 5.8^0, while the average contact angle of hydrophilic nanofibers was (Figure 4.30A) 56.86 ± 6.2^0 (Figure 4.30B).

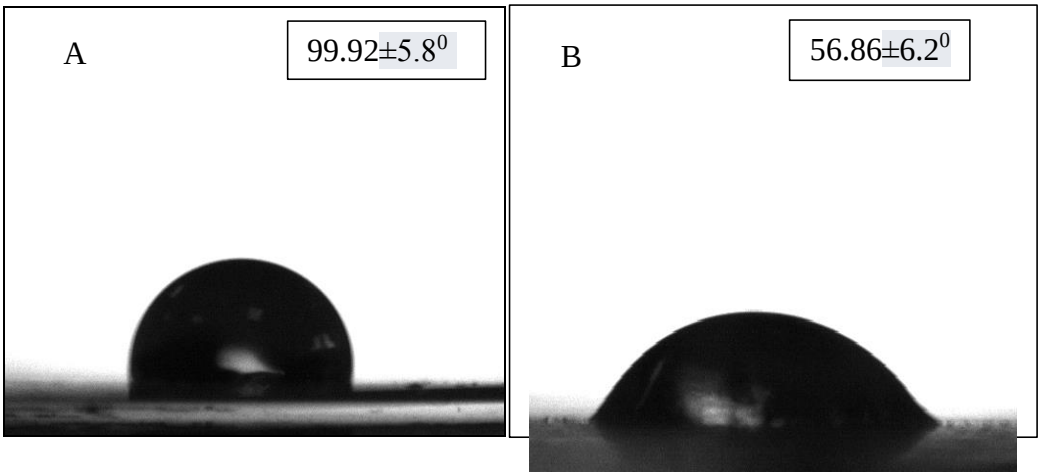

Figure 4.29. Water contact angle tests of nanofibers; A: hydrophobic nanofibers, B: hydrophilic nanofibers.

As expected, because of the hydrophobic-hydrophobic interaction, TRITC-extravidin was adsorbed on the non-biotinylated hydrophobic nanofibers that were electrospun from **(15)** (Figure 4.29A) whereas extravidin was not adsorbed on the more hydrophilic nanofibers that were electrospun from **(17)** (Figure 4.29B). Because of PEG units, nanofibers had anti-biofouling property that prevents nonspecific adsorption of extravidin. Therefore, nanofibers that contained PEG unit were used for bioimmobilization. These nanofibers were treated with 20 µl DIBO-Biotin (1mg/1mL) for 6 h in the dark and after rinsing unbound biotin, treated with 15 µl TRITC-Extravidin (1 mg/100 mL) for 0.5 h in the dark (4.31A). The immobilization was confirmed with a red color under fluorescence microscope. As a control, nanofibers without biotin were treated with 15 µl TRITC-extravidin (1mg/100mL) for 0.5 h and analyzed under fluorescence microscope to reveal the expected results (Figure 4.31B). The control experiment did not give any fluorescence indicating that the conjugation was due to the strain promoted azide-alkyne cycloaddition.

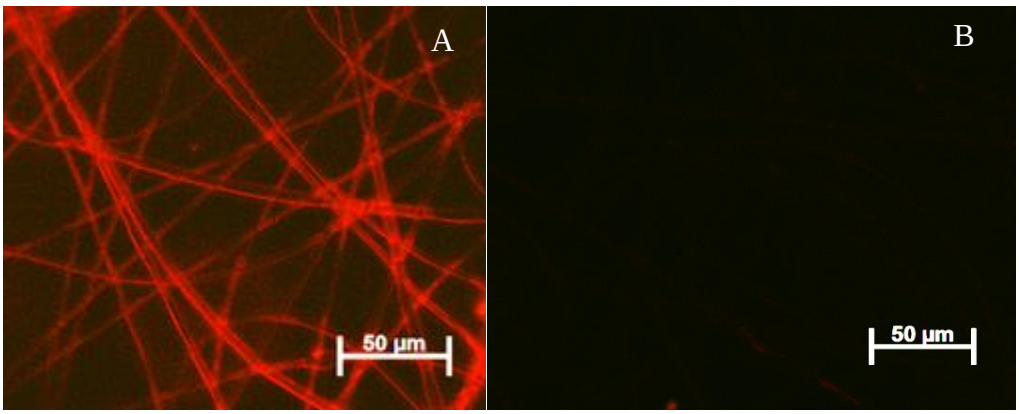

Figure 4.30. Fluorescence images of TRITC-extravidin conjugated nanofibers; A: Biotinylated nanofibers, B: Control experiment without biotin.

5. CONCLUSIONS

Novel bio-functionalizable ‘clickable’ polyester nanofibers were designed that could be functionalized without the need for metal catalysts that are often toxic to living cells. An azide-containing carbonate monomer was synthesized for enabling functionalization of nanofibers. Lactide and azide-containing carbonate monomer were copolymerized via organo-catalyzed ring opening polymerization. DBU and TU were used to catalyze the benzyl alcohol initiated polymerization. Polymers with different azide contents were synthesized to evaluate tunability of functionalization of nanofibers. Azide-containing nanofibers and FITC-cycloalkyne were combined via strain-promoted azide alkyne cycloaddition to investigate nanofiber functionalization. The work was extended to protein immobilization. DIBO-biotin was attached to the azide containing nanofibers via strain-promoted azide alkyne cycloaddition and then TRITC-extravidin was immobilized to the biotinylated nanofibers. Overall, ‘clickable’ polyester nanofibers were generated that can be used for bioimmobilization; an important step that is needed for fabrication of sensing platforms utilized in a variety of medical diagnostics.

APPENDIX A

GPC chromatograms, FTIR spectrums and SEM images are included.

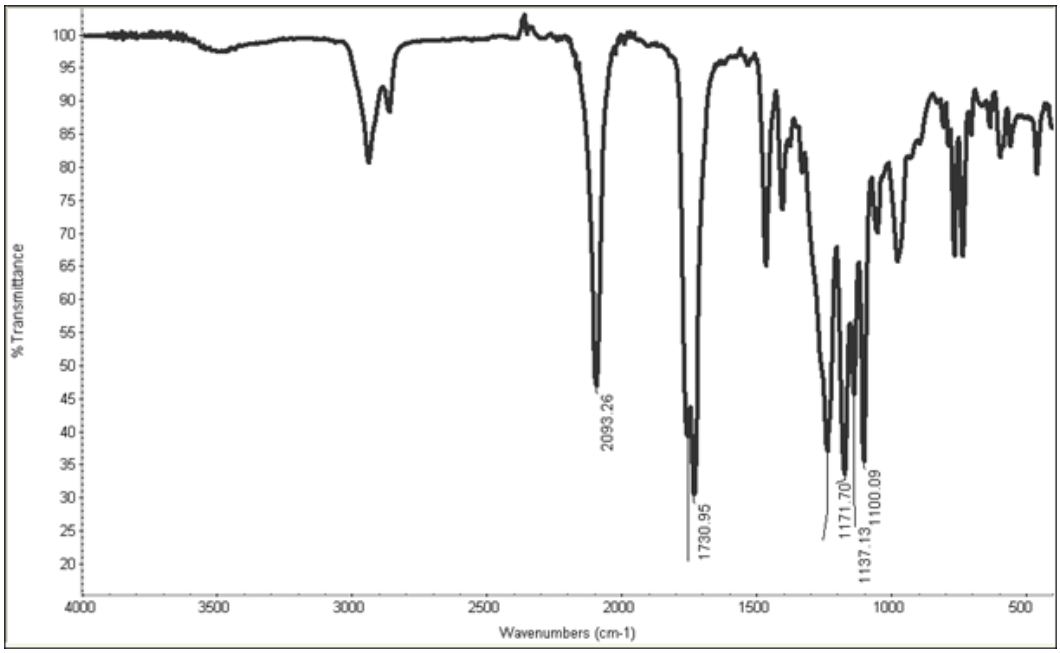

Figure A.1. FTIR spectrum of azide-containing carbonate monomer **(13)**.

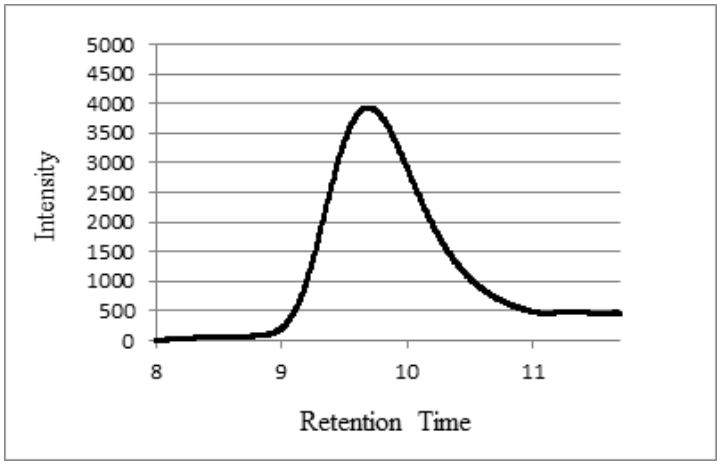

Figure A.2. GPC chromatogram of 5% azide containing copolymer **(14)**.

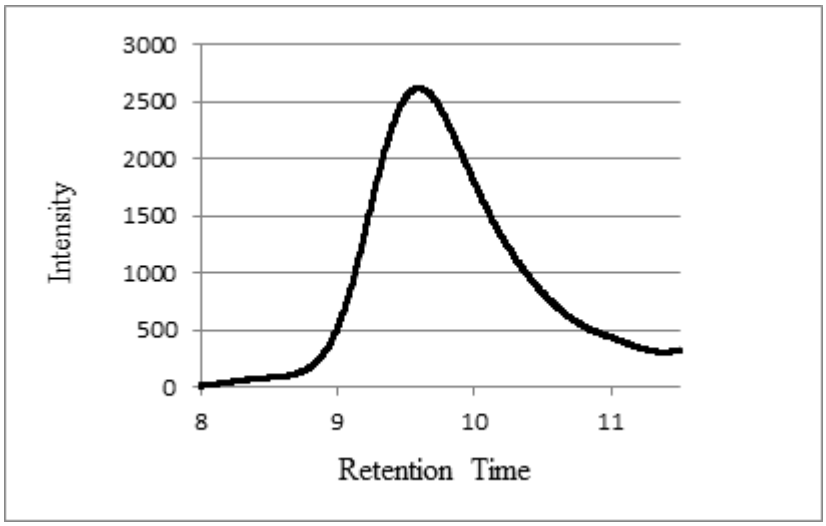

Figure A.3. GPC chromatogram of 10% azide containing copolymer **(15)**.

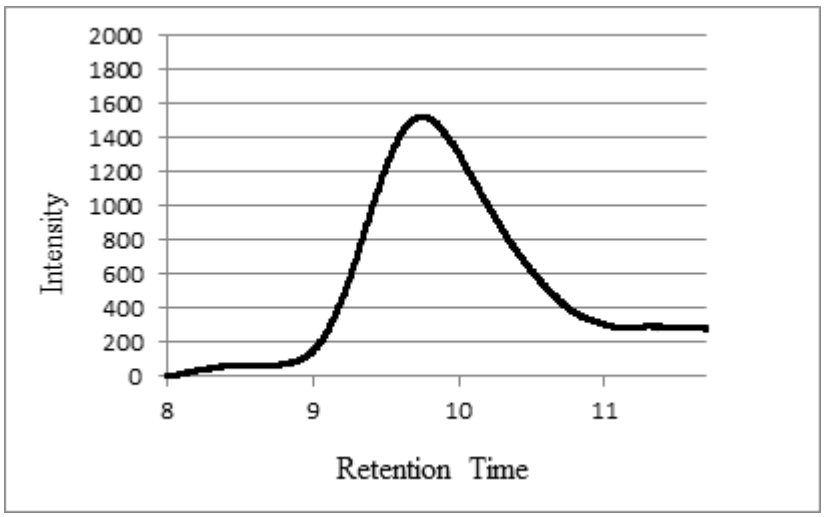

Figure A.4. GPC chromatogram of 20% azide containing copolymer **(16)**.

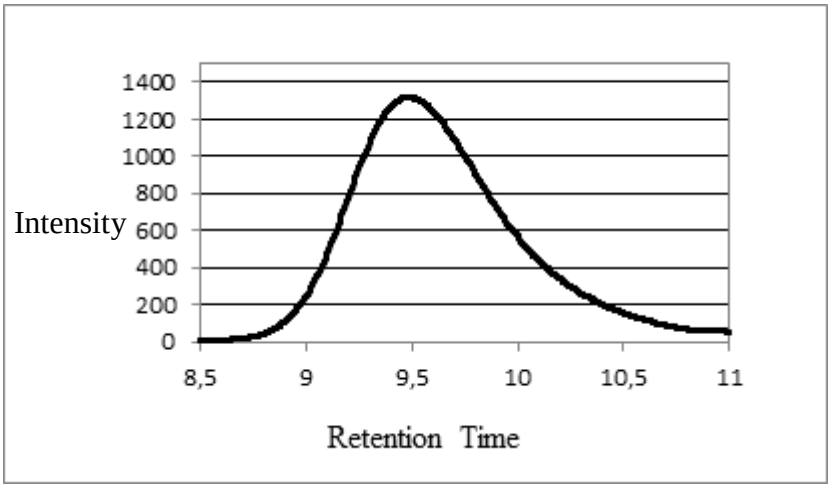

Figure A.5. GPC chromatogram of copolymer **(17)**.

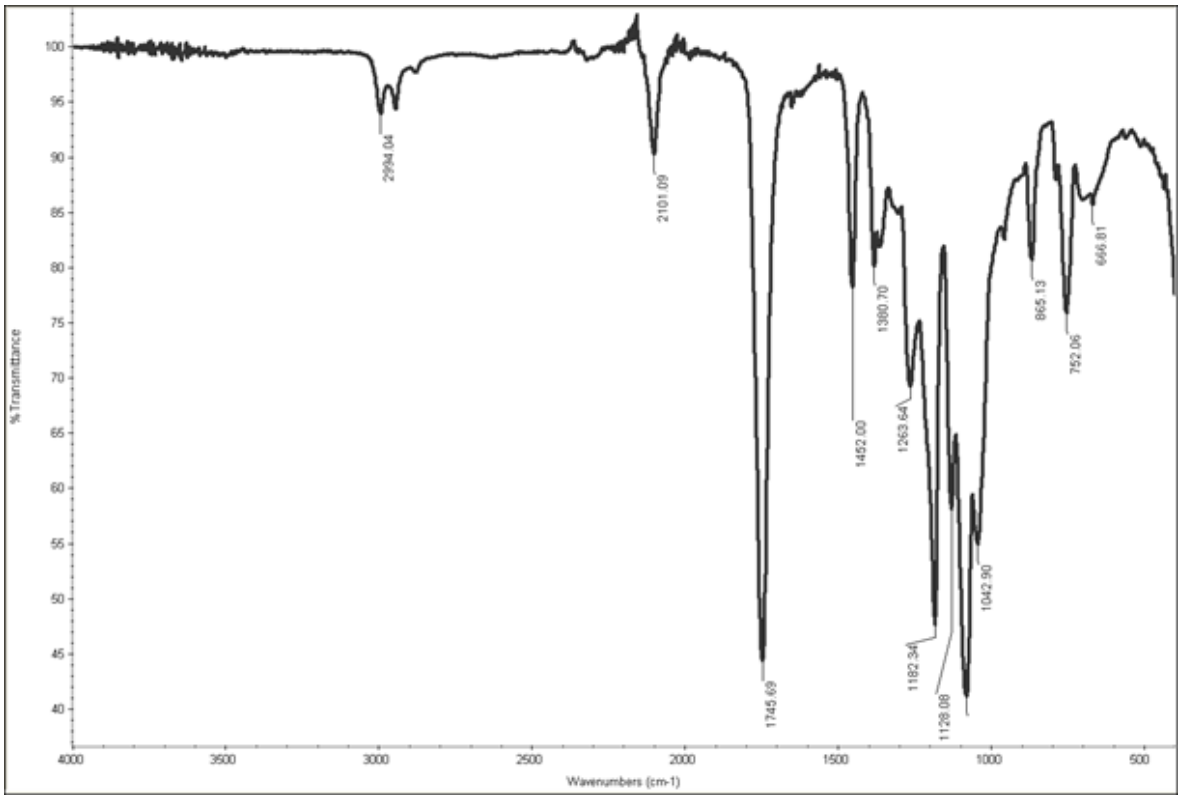

Figure A.6. FTIR spectrum of azide containing copolymer **(17)**.

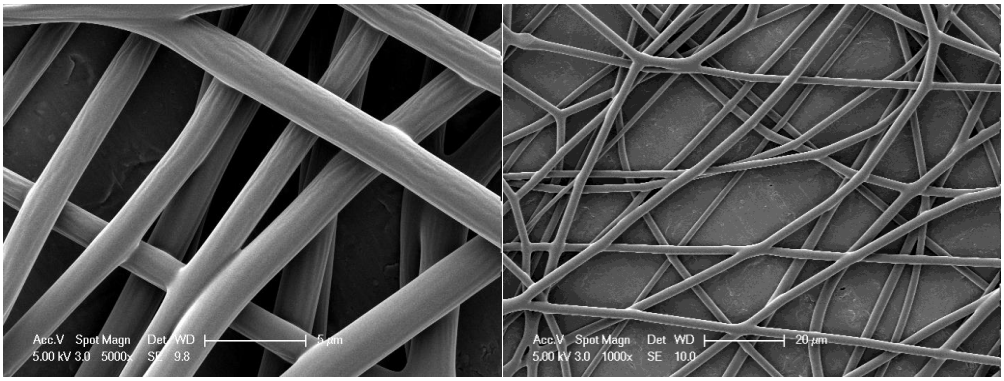

Figure A.7. SEM images of fibers, 58 wt % polymer in chloroform.

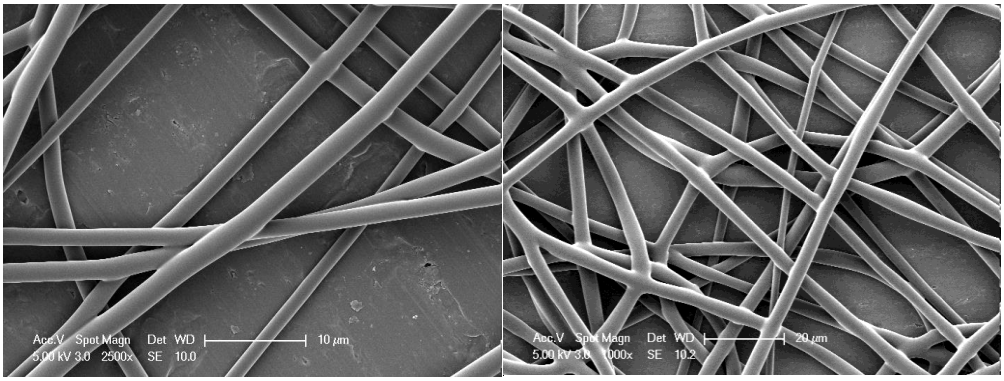

Figure A.8. SEM images of nanofibers, 50 wt % polymer in chloroform.

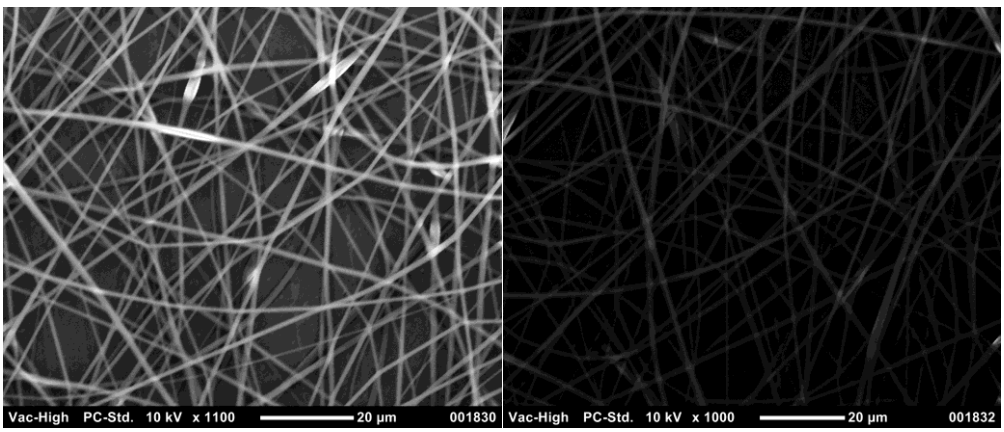

Figure A.9. SEM images of nanofibers, 43 wt % polymer in chloroform.

REFERENCES

1. Ulery, B.D., L.S. Nair, and C.T. Laurencin, "Biomedical Applications Of Biodegradable Polymers", *Journal of Polymer Science, Part B: Polymer Physics*, Vol. 49, pp. 832–864, 2011.

2. Hernández-Vargas, J., J.B. González-Campos, J. Lara-Romero, and J.M. Ponce-Ortega, "A Mathematical Programming Approach For The Optimal Synthesis Of Nanofibers Through An Electrospinning Process", *ACS Sustainable Chemistry & Engineering*, Vol. 2, pp. 454–464, 2014.

3. Liang, D., B.S. Hsiao, and B. Chu, "Functional Electrospun Nanofibrous Scaffolds For Biomedical Applications", *Advanced Drug Delivery Reviews*, Vol. 59, pp. 1392–1412, 2007.

4. Gouma, P.I., "Nanostructured Polymorphic Oxides For Advanced Chemosensors", *Reviews on Advanced Materials Science*, Vol. 5, pp. 147–154, 2003.

5. Jing, X., M.R. Salick, T. Cordie, H. Mi, X. Peng, and L. Turng, "Electrospinning Homogeneous Nano Fi Brous Poly (Propylene Carbonate)/ Gelatin Composite Sca Ff Olds For Tissue Engineering" 2014.

6. Huang, Z.M., Y.Z. Zhang, M. Kotaki, and S. Ramakrishna, "A Review On Polymer Nanofibers By Electrospinning And Their Applications In Nanocomposites", *Composites Science and Technology*, Vol. 63, pp. 2223–2253, 2003.

7. Yao, J., C. Bastiaansen, and T. Peijs, "High Strength And High Modulus Electrospun Nanofibers", *Fibers*, Vol. 2, pp. 158–186, 2014.

8. Buchko, C.J., K.M. Kozloff, and D.C. Martin, "Surface Characterization Of Porous, Biocompatible Protein Polymer Thin Films", *Biomaterials*, Vol. 22, pp. 1289–1300, 2001.

9. Li, Z., and C. Wang, "Effects Of Working Parameters On Electrospinning", *One-Dimensional nanostructures*, pp. 15–29, 2013.

10. Deitzel, J.., J. Kleinmeyer, D. Harris, and N.. Beck Tan, "The Effect Of Processing Variables On The Morphology Of Electrospun Nanofibers And Textiles", *Polymer*, Vol. 42, pp. 261–272, 2001.

11. Yu, L.Yu., H.M. Shen, and Z.L. Xu, "PVDF–TiO2 Composite Hollow Fiber Ultrafiltration Membranes Prepared By TiO2 Sol–Gel Method And Blending Method", *Journal of Applied Physics*, Vol. 113, pp. 1763–1772, 2009.

12. Fong, H., I. Chun, and D.H. Reneker, "Beaded Nanofibers Formed During Electrospinning", *Polymer*, Vol. 40, pp. 4585–4592, 1999.

13. Yang, Q., Z. Li, Y. Hong, Y. Zhao, S. Qiu, C. Wang, and Y. Wei, "Influence Of Solvents On The Formation Of Ultrathin Uniform Poly(vinyl Pyrrolidone) Nanofibers With Electrospinning", *Journal of Polymer Science Part B: Polymer Physics*, Vol. 42, pp. 3721–3726, 2004.

14. Reneker, D.H., and I. Chun, "Nanometre Diameter Fibres Of Polymer, Produced By Electrospinning", *Nanotechnology*, Vol. 7, pp. 216–223, 1999.

15. Zhang, C., X. Yuan, L. Wu, Y. Han, and J. Sheng, "Study On Morphology Of Electrospun Poly(vinyl Alcohol) Mats", *European Polymer Journal*, Vol. 41, pp. 423–432, 2005.

16. Yuan, X.Y., Y.Y. Zhang, C. Dong, and J. Sheng, "Morphology Of Ultrafine Polysulfone Fibers Prepared By Electrospinning", *Polymer International*, Vol. 53, pp. 1704–1710, 2004.

17. Kalaoglu-Altan, O.I., R. Sanyal, and A. Sanyal, "'Clickable' Polymeric Nanofibers Through Hydrophilic–Hydrophobic Balance: Fabrication Of Robust Biomolecular Immobilization Platforms", *Biomacromolecules*, Vol. 16, pp. 1590–1597, 2015.

18. Ki, C.S., D.H. Baek, K.D. Gang, K.H. Lee, I.C. Um, and Y.H. Park, "Characterization Of Gelatin Nanofiber Prepared From Gelatin–formic Acid Solution", *Polymer*, Vol. 46, pp. 5094–5102, 2005.

19. Dechy-Cabaret, O., B. Martin-Vaca, and D. Bourissou, "Controlled Ring-opening Polymerization Of Lactide And Glycolide", *Chemical Reviews*, Vol. 104, pp. 6147–6176, 2004.

20. Zhao, Y.C., D. Zhou, Q. Chen, X.J. Zhang, N. Bian, A. Di Qi, and B.H. Han, "Thionyl Chloride-catalyzed Preparation Of Microporous Organic Polymers Through Aldol Condensation", *Macromolecules*, Vol. 44, pp. 6382–6388, 2011.

21. Refojo, M.F., "Application of Materials in Medice and Dentistry: Ophthalmologic Applications", *Biomaterials Science - An Introduction to Materials in Medicine* 1996.

22. Kennedy, J., and M. Thorley, "Polymers And The Environment", *Carbohydrate Polymers*, Vol. 42, pp. 427, 2000.

23. Onbulak, S., S. Tempelaar, R.J. Pounder, O. Gok, R. Sanyal, A.P. Dove, and A. Sanyal, "Synthesis And Functionalization Of Thiol-Reactive Biodegradable Polymers", *Macromolecules*, Vol. 45, pp. 1715–1722, 2012.

24. Dubois, P., O. Coulembier, and J.M. Raquez, "Handbook of Ring-Opening Polymerization", *Wiley-VCH Verlag GmbH & Co, KGaA*2009.

25. Nuyken, O., and S. Pask, "Ring-Opening Polymerization—An Introductory Review", *Polymers*, Vol. 5, pp. 361–403, 2013.

26. Labet, M., and W. Thielemans, "Synthesis Of Polycaprolactone: A Review", *Chemical Society Reviews*, Vol. 38, pp. 3484, 2009.

27. Wang, L., V. Poirier, F. Ghiotto, M. Bochmann, R.D. Cannon, J.F. Carpentier, and Y. Sarazin, "Kinetic Analysis Of The Immortal Ring-opening Polymerization Of Cyclic Esters: A Case Study With Tin(II) Catalysts", *Macromolecules*, Vol. 47, pp. 2574–2584, 2014.

28. Bhaw-Luximon, A., D. Jhurry, S. Motala-Timol, and Y. Lochee, "Polymerization Of Epsilon-caprolactone And Its Copolymerization With Gamma-butyrolactone Using Metal Complexes", *Macromolecular Symposia*, Vol. 231, pp. 60–68, 2006.

29. Nederberg, F., E.F. Connor, M. Möller, T. Glauser, and J.L. Hedrick, "New Paradigms For Organic Catalysts: The First Organocatalytic Living Polymerization The Authors Would Like To Thank The NSF Center On Polymer Interfaces And Macromolecular Assemblies (CPIMA). T.G. Expresses His Thanks To The Swiss Academy Of Engineering ", *Angewandte Chemie (International ed. in English)*, Vol. 40, pp. 2712–2715, 2001.

30. Lohmeijer, B.G.G., R.C. Pratt, F. Leibfarth, J.W. Logan, D. a. Long, A.P. Dove, F. Nederberg, J. Choi, C. Wade, R.M. Waymouth, and J.L. Hedrick, "Guanidine And Amidine Organocatalysts For Ring-opening Polymerization Of Cyclic Esters", *Macromolecules*, Vol. 39, pp. 8574–8583, 2006.

31. Martin, O., and L. Avérous, "Poly(lactic Acid): Plasticization And Properties Of Biodegradable Multiphase Systems", *Polymer*, Vol. 42, pp. 6209–6219, 2001.

32. Maharana, T., B. Mohanty, and Y.S. Negi, "Melt-solid Polycondensation Of Lactic Acid And Its Biodegradability", *Progress in Polymer Science (Oxford)*, Vol. 34, pp. 99–124, 2009.

33. Joshi, J. a Y.R., and R.P. Patel, "Role Of Biodegradable Polymers In Drug Delivery", *International Journal of Current Pharmaceutical Research*, Vol. 4, pp. 74–81, 2012.

34. Daniel Taton, Y.G., "Controlled Polymerizations As Tools For The Design Of Star-like And Dendrimer-like Polymers", *Polymer international*, Vol. 1370, pp. 1361–1370, 2006.

35. Kolb, H.C., M.G. Finn, and K.B. Sharpless, "Click Chemistry: Diverse Chemical Function From A Few Good Reactions", *Angewandte Chemie (International ed. in English)*, Vol. 40, pp. 2004–2021, 2001.

36. Huisgen, R., "Kinetics And Mechanism Of 1,3-Dipolar Cycloadditions", *Angewandte Chemie International Edition in English*, Vol. 2, pp. 633–645, 1963.

37. Gregory C. Patton, "Development And Applications Of Click Chemistry", pp. 57–64, 2004.

38. Lin, F., J. Yu, W. Tang, J. Zheng, S. Xie, and M.L. Becker, "Postelectrospinning 'Click' Modi Fi Cation Of Degradable Amino Acid- Based Poly(ester Urea) Nano Fibers" 2013.

39. Agard, N.J., J. a Prescher, and C.R. Bertozzi, "A Strain-promoted [3 + 2] Azide-alkyne Cycloaddition For Covalent Modification Of Biomolecules In Living Systems", *Journal of the American Chemical Society*, Vol. 126, pp. 15046–7, 2004.

40. Himo, F., T. Lovell, R. Hilgraf, V. V. Rostovtsev, L. Noodleman, K.B. Sharpless, and

V. V. Fokin, “Copper(I)-catalyzed Synthesis Of Azoles. DFT Study Predicts Unprecedented Reactivity And Intermediates”, *Journal of the American Chemical Society*, Vol. 127, pp. 210–216, 2005.

41. Rock, J.M., D. Lim, L. Stach, R.W. Ogrodowicz, J.M. Keck, M.H. Jones, C.C.L. Wong, J.R. Yates, M. Winey, S.J. Smerdon, M.B. Yaffe, and A. Amon, “Activation Of The Yeast Hippo Pathway By Phosphorylation-dependent Assembly Of Signaling Complexes”, *Science (New York, N.Y.)*, Vol. 340, pp. 871–5, 2013.

42. Zheng, J., K. Liu, D.H. Reneker, and M.L. Becker, “Post-assembly Derivatization Of Electrospun Nanofibers Via Strain-promoted Azide Alkyne Cycloaddition”, *Journal of the American Chemical Society*, Vol. 134, pp. 17274–17277, 2012.

43. Ihre, H., A. Hult, and E. Söderlind, “Synthesis, Characterization, And 1H NMR Self-diffusion Studies Of Dendritic Aliphatic Polyesters Based On 2,2-bis(hydroxymethyl)propionic Acid And 1,1,1-tris(hydroxyphenyl)ethane”, *Journal of the American Chemical Society*, Vol. 118, pp. 6388–6395, 1996.

44. Al-Azemi, T.F., and K.S. Bisht, “One-step Synthesis Of Polycarbonates Bearing Pendant Carboxyl Groups By Lipase-catalyzed Ring-opening Polymerization”, *Journal of Polymer Science: Part A: Polymer Chemistry*, Vol. 40, pp. 1267–1274, 2002.

45. Ng, V.W.L., J.P.K. Tan, J. Leong, Z.X. Voo, J.L. Hedrick, and Y.Y. Yang, “Antimicrobial Polycarbonates: Investigating The Impact Of Nitrogen-containing Heterocycles As Quaternizing Agents”, *Macromolecules*, Vol. 47, pp. 1285–1291, 2014.

46. Pratt, R.C., B.G.G. Lohmeijer, D. a. Long, P.N.P. Lundberg, A.P. Dove, H. Li, C.G. Wade, R.M. Waymouth, and J.L. Hedrick, “Exploration, Optimization, And Application Of Supramolecular Thiourea−Amine Catalysts For The Synthesis Of Lactide (Co)polymers”, *Macromolecules*, Vol. 39, pp. 7863–7871, 2006.

47. Kali, G., T.K. Georgiou, B. Iván, and C.S. Patrickios, “Anionic Amphiphilic End-Linked Conetworks By The Combination Of Quasiliving Carbocationic And Group Transfer Polymerizations”, *Journal of Polymer Science Part a-Polymer Chemistry*, Vol. 47, pp. 4289–4301, 2009.cc